DETAILED ANALYSIS OF PRESSURE DROP IN A LARGE DIAMETER VERTICAL PIPE

A

THESISPRESENTED TO THE DEPARTMENT OF

PETROLEUM ENGINEERING

AFRICAN UNIVERSITY OF SCIENCE AND TECHNOLOGY

IN PARTIAL FULFILLMENT OF THE REQUIREMENTS

FOR THE DEGREE OF

MASTER OF SCIENCE

By

NWACHUKWU KIZITO CHIBUIKE, B.Eng.(Hons.)

Abuja, Nigeria

December 2014

DETAILED ANALYSIS OF PRESSURE DROP IN A LARGE DIAMETER VERTICAL PIPE

By

NWACHUKWU KIZITO CHIBUIKE, B.Eng.(Hons.)

A THESIS APPROVED BY THE PETROLEUM ENGINNERING DEPARTMENT

RECOMMENDED: ……

Supervisor, Dr. Mukhtar Abdulkadir

……..

Head, Department of Petroleum Engineering

APPROVED: …….....

Chief Academic Officer

…….

Date

ABSTRACT

With the ever increasing need to optimize production, the accurate understanding of the mechanics of multi-phase flow and its effect on the pressure drop along the oil-well flow string is becoming more pertinent. The efficient design of gas-lift pump, electric submersible pumps, separators, flow strings and other production equipment depends on the accurate prediction of the pressure drop along the flow pipe. Pressure is the energy of the

reservoir/well and it is crucial to understand how a change in fluid properties, flow conditions and pipe geometric properties affect this important parameter in the oil and gas industry.

Extensive work on this subject has been done by numerous investigators albeit in small diameter pipes. Reliance on the empirical correlations from this investigators has been somewhat misleading in modelling pressure drop in large diameter pipes (usually >100 mm) because of the limitations imposed by the diameter at which they were developed and the range of data and conditions used in deriving them.

In this work, experimental data from the experimental study by Dr. Mukhtar Abdulkadir was used as the data source. The gas velocities, liquid velocities, film fraction, gas and liquid properties and the pipe geometric properties from the above mentioned experiment were used to model the frictional and total pressure drop from six correlations. Results were analyzed and compared with the experimental results.

ACKNOWLEDGEMENT

I would like to thank in a special way my sister and mentor Engr. Angela Nwachukwu, without her I won't be here. She has shown more than a sister's love to me and I will be forever indebted to her. I appreciate my dearest mum Mrs. Rose Nwachukwu and all my siblings for being there for me always.

I want to use this opportunity to express my gratitude to Dr. Mukhtar Abdulkadir for his continuous support and motivation throughout this work. His guidance was invaluable to the

success of this work. My appreciations also goes to all the lecturers for helping me in one way or the other in acquiring the bank of knowledge and information required in accomplishing this task.

I appreciate the support from all AUST students, all the masters and PhD students. Special mention goes to Azeko Salifu Tahiru who assisted me in using the statistical software, Minitab-16, used in some of my analysis and Bruno S. Dandogbessi for his numerous advices. The friendship and support I got from all of you kept me going.

DEDICATION

This work is dedicated to the almighty God without whom nothing is possible. I also dedicate this to my lovely family for their support and encouragement.

TABLE OF CONTENTS

CHAPTER ONE

INTRODUCTION

1.1 General introduction

Profitable production of oil and gas fields relies on accurate prediction of the multi-phase well flow. The determination of flowing bottom-hole pressure (BHP) in oil wells is very important to petroleum engineers. It helps in designing production tubing, determination of artificial lift requirements and in many other production engineering aspects such as avoiding producing a well below its bubble point in the sand-face to maintain completion stability around the

wellbore **(Ahmed, 2011).** Well fluids above bubble point pressure exist as a single phase as it is being produced from the reservoir. However, as they navigate their way through the network of interconnected pores in the reservoir to the wellbore, there is a continuous reduction in pressure as overburden stress is gradually reduced. This phenomenon leads to the liberation of the entrained gas. As the single-phase fluid rises in the tubing, a critical point is reached where some of the gases begin to come out of solution along the length of the pipe. In other words, it changes from single-phase flow to multi-phase flow.

This leads to some level of complexity as regards to the identification of the physical properties of the individual phases, the flow pattern, the relative volume occupied by the separate phases inside the pipe, and most importantly the implication of the phase separation on the pressure drop along the well tubing string.

Although most if not all calculations for flow lines in multiphase production systems have been and continue to be based on empirical correlations, there is now a strong tendency to introduce more physically based (so called mechanistic) approaches to supplement if not replace correlations. This is because the latter are well known for their unreliability when applied to systems operating under conditions different to those from which the correlations are derived; such conditions encompass: pressure, temperature, fluid properties and pipe diameter. Furthermore, correlations exist for limited geometrical configurations (i.e. vertical or horizontal pipes) and simple physical phenomena (no mass transfer between phases, constant temperature, etc.). With the advent of more complex production systems involving deviated wells as well as the move to exploit gas condensate resources the production of which will inevitably involve strong mass transfer effects, calculation methods will be required to account for such complexities. The use or extension of existing correlations to

such systems will therefore be fraught with uncertainties if at all possible **(Issa and Tang, 1991).**

Petroleum Engineers need to predict pressure drops in oil and gas wells for the following reasons:

1) To construct "lift-curves", which are tables or plots of flow-rate versus bottom hole-pressure, used to predict well flow-rates.

2) To select the appropriate tubing size. If the tubing diameter is too large, the well acts as a gas-liquid separator and a flow conduit, and the excessive slippage results in needlessly high bottom hole pressures. However, tubing which is too small will cause excessive frictional pressure drops.

3) To design artificial lift completions such as electric submersible pumps, jet pumps or gas lift.

(Pucknel- et al, 1993).

Pressure drop along the vertical tubing comes in two main components:

- Frictional drop and
- Hydrostatic drop

The acceleration component of the pressure drop is usually negligible in adiabatic flows, and hence would not be considered in this work.

In the lower portion of the flow string pressure drop due to gravity is much more predominant, meanwhile frictional pressure drop accounts for most of the total pressure drop

a column of multiphase fluid experiences along any flow conduit in the annular flow regime**.** Though this is particularly valid for small diameter pipes.

The ability to predict the variation of pressure with elevation along the length of tubing for known conditions of flow would provide a means of evaluating the effects of tubing size, flow rates and a host of other variables on flowing wells and would be particularly useful in designing gas-lift installations **(Poettmann & Carpenter, 1952).**

Considerable work has been done on the laws governing the multiphase flow of liquid and gas mixtures in vertical pipes but no satisfactory solution has been found applicable to flowing oil wells and gas-lift wells. There has been a lot of investigation on small diameter pipes but there exist a lack of experimental data in large diameter vertical pipes, i.e., in pipe sizes similar or close to those typical of industry applications and especially on important parameters such as pressure drop which is known as a key design parameter. Many empirical correlations have been developed in the past from the experimental data for predicting two-phase pressure gradient which differ in the manner used to calculate these three components above of the total pressure drop (Hewitt, 1982a, Brill and Beggs, 1991 and Azzopardi, 2006). It is worth mentioning that even with many empirical correlations and models that are available in literature they appear not to be valid over a very wide range of gas and liquid flow rates, physical properties and pipe diameters. Therefore researchers normally test the performance of these methods of prediction with the experimental data that are available to them.

1.2 Problem statement

With a plethora of correlations trying to model the two-phase flow of oil and gas wells through a conduit, it is pertinent to know the ones that come close to the actual physical measurements. The main drive in this work is to:

- Analyze the data on the experiment carried out by Mukhtar Abdulkadir which comprises of total pressure drop, liquid film fraction and gas and liquid superficial velocities.
- Compare the total pressure drop extracted from this experimental data with the frictional pressure drop calculated from selected empirical correlations.

1.3 Aims and Objectives

1.3.1 Aim

The aim of the study is to carry out a detailed analysis of pressure drop in a large diameter vertical pipe.

1.32 Objective

To achieve this aim, the following objectives will be met:

- To obtain raw experimental data concerned with total pressure drop on churn-annular flows in 127 mm diameter, 11 m length vertical pipe over a wide range of gas and liquid superficial velocities. This will be achieved by processing raw data obtained from an experiment conducted by Dr. Mukhtar Abdulkadir.
- To compare the data obtained with those available in the literature for smaller pipes so as to investigate the effect of pipe diameter on total pressure drop.
- To analyses the frictional pressure drops correlations of various investigators. The correlations chosen for the analysis include Poettmann and Carpenter (1952), Beggs and Brill (1973), Friedel (1979), modified Hagedorn and Brown (1964), Baxendel and Thomas (1961) and Chisholm (1973) frictional pressure drop correlations.
- To make a comparison between the predicted pressure drop and that obtained from experimental observation (measured pressure drop) using various statistical analysis techniques.

1.4 Structure of the thesis

- Chapter provides the introduction, the aims and objectives of this work
- Chapter two of this thesis provides a review of some important literatures on this topic. It provides the methods and procedure in which different authors and investigators looked at flow dynamics in vertical multi-phase flow as regards to pressure drop prediction.

- Chapter three focuses on the experimental/design techniques carried out based on the experiment carried out by Dr. Mukhtar Abdulkadir on 127mm (0.127m) diameter, 11 m vertical pipe. It shows the procedure that was taken in deriving the total pressure drop, the void fraction (film fraction) for each liquid and gas flow-rates. Finally, in chapter three pressure drop using different correlations were determined as an alternative to experimental technique. This is important for comparative purposes and to determine the best correlation that would fit the conditions at which the experiment was carried out.
- Chapter four shows all the analysis carried out to compare the pressure drop derived from experiment with the pressure drop from selected pressure drop correlations. Various forms of statistical analysis techniques were used to compare and contrast the pressure drop correlations in order to determine the best out of the lot.
- Chapter five is conclusion and recommendation.

CHAPTER TWO

LITERATURE REVIEW

2.1 Introduction

The prediction of pressure drop in two-phase flow in vertical tubing has received numerous attention from several investigators. Most of the correlations developed, unfortunately, are limited in their application due to the range of data used in deriving them. And currently there is scarcity of correlations in literature on pipes with diameter greater than 100 mm but a look

at the correlations on smaller diameter pipes can give us a hint on the effect of pipe diameter on two-phase pressure drop in vertical pipes.

Aziz et al (2001), developed a sound mechanistically-based prediction method for the flow pattern encountered in oil wells- those where the oil is the continuous phase, i.e., the single phase, the bubble and slug flow patterns. They argued that all methods for the prediction of the relationship between the pressure gradient, the flow rates, the fluid properties and the geometry of the flow duct involve one form or another of the mechanical energy equation. For a small elevation change, ΔZ, the equation maybe written as equation (2.111).

They developed a calculation method with the concept described. The proposed method, based on mechanical considerations, permit ready identification of the flow pattern, and the calculation of the in-situ void fraction of the gas phase and the pressure gradient.

The predicted pressure drop compares favorably with measured values in 44 of the 48 wells for which adequate data are reported.

Hagedorn and Brown (1964) method is based on data obtained from a 1500 feet deep vertical experimental well. Air was the gas phase and four different liquids were used: water and crude oil of viscosities of about 10, 30 and 110 cP. Tubing of about 1.0, 1.25 and 1.5 in. nominal diameters were used. However, Hagedorn and Brown (1964) did not measure liquid hold-up, rather they developed a pressure gradient equation that, after assuming a friction-factor correlation permitted the calculation of pseudo liquid hold-up values for each test to match measured pressure gradients.

Hagedorn and Brown developed a pressure gradient for vertical multi-phase flow using equation (2.115).

Gray (1978) developed a method to determine pressure gradient in a vertical well that also produces condensate fluids or water. A total of 108 well-test data were used to develop the empirical correlation. Of these sets, 88 were obtained on wells reportedly producing free liquids.

Gray proposed equation (2.115) to predict pressure gradient for two-phase flow in a vertical gas well.

Fancher et al (1963) developed a correlation which is based on Poettmann and Carpenter (1952)'s method. An energy balance between any two points in the flow string in which the flowing fluid was treated as a single homogeneous fluid was developed as a basis for their correlation. The irreversible energy losses were incorporated in a Fanning-type friction factor term. A correlation was developed by back-calculating the friction term from field data and plotting it against the numerator of the Reynolds number. Viscosity effects were not included

in their correlation due to the high degree of turbulence of both phases. Viscous shear is negligible if both phases are in high degree of turbulence.

In their work, the original **Poettmann and Carpenter** (1952) correlation was extended to cover the lower density ranges (in particular less than 10 lb. /cu-Ft. for 2-inch tubing), which Poettmann stated was outside the range of their original data. This lower density range was further correlated by using the producing gas-liquid-ratio as an additional parameter.

The irreversible energy loss term was evaluated by calculation using field data to determine the pressure gradient from equation (2.117)

They plotted the fanning-type friction factor against the numerator of the Reynolds number. The scattering of points in this correlation shows that an important parameter(s) was/were neglected. They then employed the gas-liquid-ratio as an additional parameter, and a correlation was developed between the Fanning friction factor and the numerator of the Reynolds number for three ranges of gas-liquid-ratios.

In comparing their correlation to that of Poettmann and Carpenter (1952), they concluded that Poettmann and Carpenter correlation shows excellent agreement at high flow rates, but results in large deviation at low flow rates and low density ranges.

Chierici et al (1974) examined the pressure drop and flow regimes in a vertical flowing oil well. Starting from the mechanical energy balance equation, they expressed the elementary pressure drop, dp, in a vertical well as follows:

By making some approximations in evaluating the acceleration gradient, VdV, which is almost negligible, equation (2.119) was obtained:

They grouped the various ways a gas-liquid mixture can flow in a vertical pipe into three main flow regimes; that is, bubble-plug flow, slug-froth flow, and mist flow. A transition flow exists between the last two flow regimes.

The frictional loss gradient, is calculated according to the classical equation;

Where the friction factor, f, is obtained by entering the Moody diagram with the appropriate N_{Re} and ε/d_h values. What density, velocity and Reynolds number are to be used depends on the flow regime mentioned above.

In their paper, **Hasan and Kabir** (1988) examined the void fractions for different flow regimes (bubbly, slug, churn and annular flow regimes), the transition criteria and the pressure gradient predictions. The void fraction and pressure gradient predictions of the theory presented in their paper for vertical up-flow of two-phase fluids are compared with published data from diverse sources. The predictions of the proposed theory were plotted against the void fraction data of Beggs and Brill (1973) for vertical systems. Beggs and Brill's data were gathered with air/water in 1.5- and 1-in. (3.8- and 2.5-cm) pipes at 4- to 7-atm (405- to 709-kPa) pressures and 50 to 100^0F (10 to 38^0F) temperatures. The agreement between the data and the prediction were excellent for all flow regimes except churn flow. Their theory appears to over-estimate void fraction during churn flow slightly, suggesting a somewhat higher value of C_1 than is usually used. However, they also observed that the highly fluctuating nature of churn flow makes accurate data gathering difficult.

Their study presents a model for predicting flow behavior of two-phase gas/oil mixtures in vertical oil wells. The major advantage of the proposed method is that it is based on the physical behavior of the flow and therefore is more reliable than available correlation under

diverse production conditions. They used data from various sources to verify the accuracy of the model.

Specifically the model is capable of predicting flow regime, void fraction, and pressure drop at any point in the flow string.

Pucknell et al (1993) evaluated two of a number of published mechanistic models – one by Ansari (1994) and the other by Hasan and Kabir (1988).

The objective of their work was to compare the Ansari and the Hasan & Kabir methods against the traditional multi-phase correlations. The following performance measures were used, based on the practical application of these models:

1) When predicted pressure drops are compared with measurements made in oil and gas fields, the multiphase model should give accurate results across the full range of producing conditions.

2) In combination with other information, the method should accurately predict when a well will cease to flow stably. In some cases, the requirements for "kicking off', adding artificial lift or recompleting with smaller tubing later in the well's life can be very important.

3) The method should not contain any discontinuities which result in sudden changes in pressure as a result of small changes in flow-rate or some other parameter.

4) The model should not be prone to numerical convergence problems.

With the oil flow-rate, water-cut, gas-oil-ratio and pressure at the wellhead readily available, they obtained a bottom-hole pressure through well-tests (just prior to pressure buildup) and production logging. The two sources of data were used in their study.

246 measurements of bottom hole flowing pressure were obtained, together with the required ancillary data, from 8 producing fields. Virtually all the data were from deviated wells with tubing of between 3 1/2" and 7".

None of these measurements was available during the development of any of the multiphase models considered, so their use represents a completely independent test.

In the result, no model gives the best results for all fields. The variability in performance can be extreme. For example, Duns and Ros (1963) gives good results in oilfield B with absolute errors of under

3%, however the same method gives an error of119% in gas field A. The results support the accepted practice of determining which correlation gives the most accurate predictions of bottom-hole pressure in each field. That method is then used to predict future field performance.

Despite the development of new mechanistic models, no single method gives accurate predictions of bottom hole flowing pressures in all fields.

Takacs (2001) examined the problem of predicting multiphase pressure drops in oil wells by analyzing the findings of all previously published evaluations. Based on these, the following main conclusions can be drawn:

- None of the available vertical multiphase pressure drop calculation models is generally applicable because their prediction errors may considerably vary in the different ranges of the flow parameters.
- There is no “over-all best” calculation method, and all efforts to find one are deemed to fail.

In spite of the claims found in the literature, the introduction of mechanistic models did not deliver a breakthrough yet because their accuracy does not substantially exceed that of the empirical ones.

Based on a sufficiently great number of experimental data from the oilfield considered, one can determine the optimum pressure drop prediction method for that field.

Reinicke et al (1987) investigated more than 15 correlations and combinations of correlations in order to identify the best method for prediction of pressure loss in deep, high-water-cut gas wells. These correlations are categorized into four groups: single-phase correlations, two-phase correlations based on the assumption that gas and liquid phases travel at the same velocity (no-slip, no-flow-regime consideration), two-phase correlations that consider slippage between the phases but no-flow regimes, and two-phase correlations that consider both slip and flow regimes.

A main program was written and the various pressure prediction methods and fluid-property correlations incorporated as subroutines. These routines were taken from published sources whenever possible (e.g., Brill and Beggs, 1973) and supplemented by routines developed in-house only where necessary. The program allows calculations from either top to bottom or bottom to top. The total length of the wellbore can be sectioned to handle changes in tubing/casing size, wellbore deviation, and pipe roughness. Each of these sections can be divided further into increments in which the pressure-gradient equation is solved for either pressure or length.

Khasanov et al (2007) developed an analytical void fraction expressions for each of the flow regime considered and used in well optimization cycle. Such expressions enable explicit

pressure versus depth dependence to be developed as soon as the proper simplifying assumption on PVT properties are made (for example, the linear dependence for solution gas-oil-ratio on pressure). The evaluation of the proposed model was performed by comparing the predicted pressure drop to the measured one according to the wells from TUFFP databank for four mechanistic models. The models involved in comparison are: Ansari mechanistic model, Unified mechanistic model, Hasan and Kabir (1988). The pressure drop was calculated with the use of the above three mechanistic model plus the proposed model. A new model for void fraction and pressure gradient prediction for vertical and slightly deviated wells was developed based on drift-flux approach. The model was evaluated using TUFFP databank as well as Rosneft field data. Evaluation showed that in comparison with mechanistic models, the proposed model enables the calculation of pressure with comparable accuracy, and less calculation resources required. Due to simplicity of void fraction expression provided by drift-flux approach, this approach allows calculating pressure gradient for a great number of wells simultaneously which is essential in production optimization.

Poettmann and (1952) in their classic paper described a method of predicting the pressure transverse of flowing oil wells and gas-lift wells. The method is based on a field data from a large number of flowing and gas-lift wells operating over a wide range of conditions. As in any correlation, there are definite limitations and range of operations to which the correlation can be applied. The correlation is based on 2-, 2 ½-, and 3-in. diameter nominal size tubing; gas-liquid ratios of up to 5,000 cu-ft. of gas per barrel of liquid; liquid rates from 60 bbl. to 1,500 total liquid per day; water-oil ratio of 56 bbl. of water per bbl. of oil; oil gravities from 30 API to 56 API; and well depths to 11,000 ft.

The procedure developed permits the calculation of the bottom-hole pressure of flowing knowing only surface data; and, in the case of gas-lift wells, it permits calculation of the depth at which to inject the gas, the pressure at which to inject the gas, the rate at which to inject the gas, the ideal horsepower requirements necessary to lift the oil, and the effect of production rate and tubing size on these quantities.

In order to establish an idea of the reliability of the correlation, they compared the overall pressure gradients with field-measured gradients. The agreement between observed and calculated results was good. The algebraic average deviation for all the data was +1.8 percent and the standard deviation from the algebraic average was 8.3 percent.

2.2 Void Fraction and Liquid Holdup

In the flow of oil well fluids from the reservoir, there is a gradual decrease in the pressure acting on the fluid. Phase separation gradually occurs as the confining pressure is gradually removed. When we have multiple phases passing through a cross-section of the pipe, each phase can obviously not cover more than a fraction of the area. If, for instance, a fourth of the cross-section is occupied by gas, we say the gas area fraction (or the volume fraction, since volume corresponds to area if the length of that volume is infinitely small) or simply the void fraction is 0.25. If the remaining area is occupied by liquid, the liquid hold-up (liquid fraction) has to be 1 - 0.25 = 0.75. The void fraction and liquid holdup is a function of the relative liquid and gas velocities and flow rates.

The void fraction along the length of the pipe varies from zero when the fluid is still in single phase to over 0.9 in annular flow. This has a significant effect on the pressure drop along the vertical flow string.

There are different correlations used in estimating void fractions

Where: Equation (2.21) clearly suggests that accurate estimation of the gas void fraction is essential to the hydrostatic head computation that accounts for most of the pressure drop - greater than 90 % at low flow rates.

2.3 Flow Regimes

When a gas and a liquid are forced to flow together inside a pipe, there are at least 7 different geometrical configurations, or *flow regimes* that are observed to occur. These spatial configurations of the gas and liquid phases affect the pressure losses along the flow string in one way or the other. The flow regime depends on the fluid properties, the size of the conduit and the flow rates of each of the phases. The flow regime can also depend on the configuration of the inlet; the flow regime may take some distance to develop and it can change with distance as (perhaps) the pressure, which affects the gas density, changes. For fixed fluid properties and conduit, the flow rates are the independent variables that when adjusted will often lead to changes in the flow regime. There is no sharp changes in the flow regime, hence there exists flow regime transitions **(McQuillen et al).**

The boundaries between the various flow patterns in a flow pattern map occur because a regime becomes unstable as the boundary is approached and growth of this instability causes transition to another flow pattern. Like the laminar-to-turbulent transition in single phase flow, these multiphase transitions can be rather unpredictable since they may depend on otherwise

minor features of the flow, such as the roughness of the walls or the entrance conditions. Hence, the flow pattern boundaries are not distinctive lines but more poorly defined transition zones (www.cco.caltech.edu/~brennen/multiph/chap7.pdf). Figure (2.31) shows the vertical flow regime map of Hewitt and Roberts (1969) for flow in a 3.2cm diameter tube, validated for both air/water flow at atmospheric pressure and steam/water flow at high pressure.

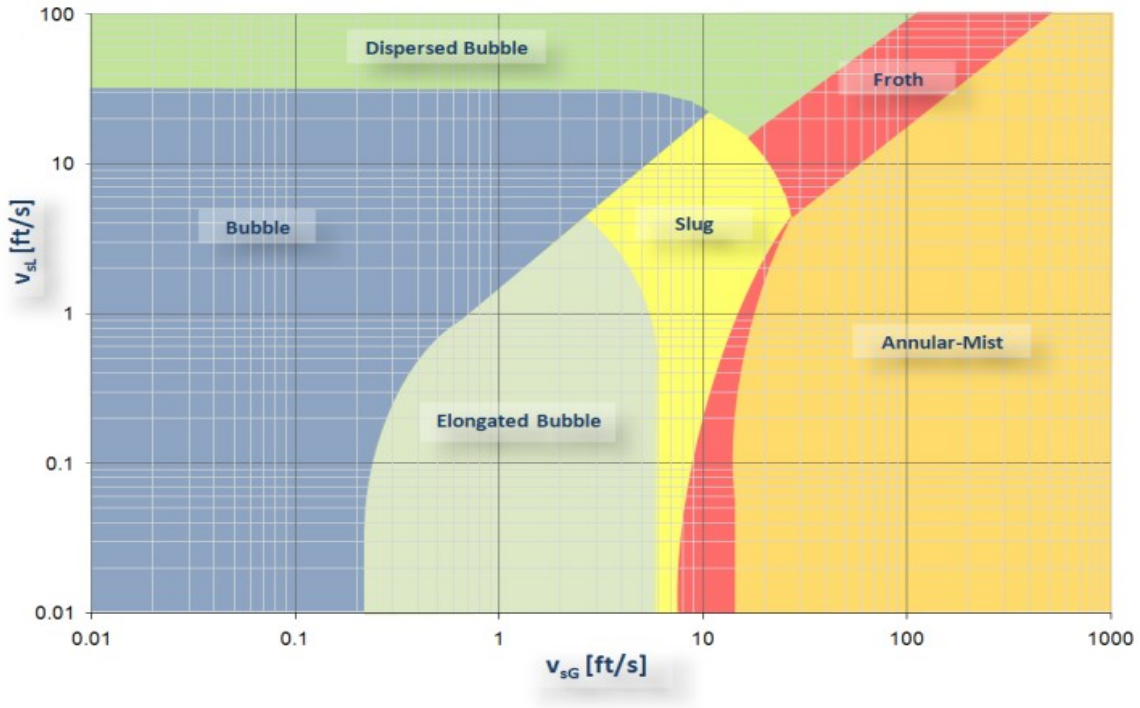

Figure (2.31): A typical flow pattern map for vertical upward gas-oil flow.

2.3.1 Bubbly flow: At low gas-fractions, the liquid is continuous and the gas exists as individual bubbles. In the bubble flow pattern, the liquid phase almost completely fills the pipe and the gas is present in the liquid as small bubbles and is randomly distributed. The diameters of the bubbles vary randomly. Also the velocities of the bubbles are different

because of the respective diameters. This type of flow occurs at low turbulence and also at relatively low liquid rates. Some authors make the distinction between homogeneous (or dispersed) and heterogeneous (or discrete) bubbly flow. Homogeneous flow occurs at low voidages, where the bubble size distribution (BSD) is narrow and there exists little interaction between bubbles, while with increasing gas-fraction the distribution broadens and bubble coalescence and break-up begin to occur. The boundary between homogeneous and heterogeneous bubbly flow is not well defined.

2.3.2 Slug flow: Slug flow is characterized by series of slug units. Each unit is composed of gas pocket called a Taylor bubble, a plug of liquid called a slug, and a film of liquid around the Taylor bubble flowing downward relative to the Taylor bubble. The Taylor bubble is an axially symmetrical, bullet-shaped gas pocket that occupies almost the pipe's entire cross-section. As the gas-fraction increases, bubble coalescence becomes more prolific and the mean bubble size increases until slugs form which approach the diameter of the column.

2.3.3 Churn flow: Churn flow is the chaotic flow of gas and liquid in which the shape of both the Taylor bubble and the liquid slugs are distorted. It results from the instability of the Taylor bubbles caused by increased void fraction and gas velocity. Neither phases appear to be continuous. The continuity of the liquid in the slug is represented by a high local gas concentration. An oscillatory or alternating direction of motion in the liquid phase is typical of churn flow. Churn flow with its characteristic oscillations is an important pattern and, often covering a fairly wide range of gas flow rate. At its higher range of gas velocity, the liquid consists mainly of a thick film on the pipe wall covered with large waves. Therefore, in that

sense the term semi-annular can be used for this flow pattern. However, researchers, e. g., Hewitt and Hall-Taylor (1970), prefer the more general term "churn" to cover the whole region.

2.3.4 Annular flow: Annular flow is characterized by axial continuity of the gas phase in a central core with the liquid flowing upwards, both as thin film along the pipe wall and as dispersed droplets in the core. At high gas flow rates more liquid become dispersed in the core, leaving a very thin liquid film flowing along the wall. According to Costigan and Whalley (1997), the annular type flow in vertical pipes occurs at gas void fractions above 0.8. The interfacial shear stress acting at the core/film interphase and the amount of entrained liquid in the core are important parameters in annular flow.

Fig (2.341) represents the geometrical configuration of the different flow regions encountered in a poly-phasic flow.

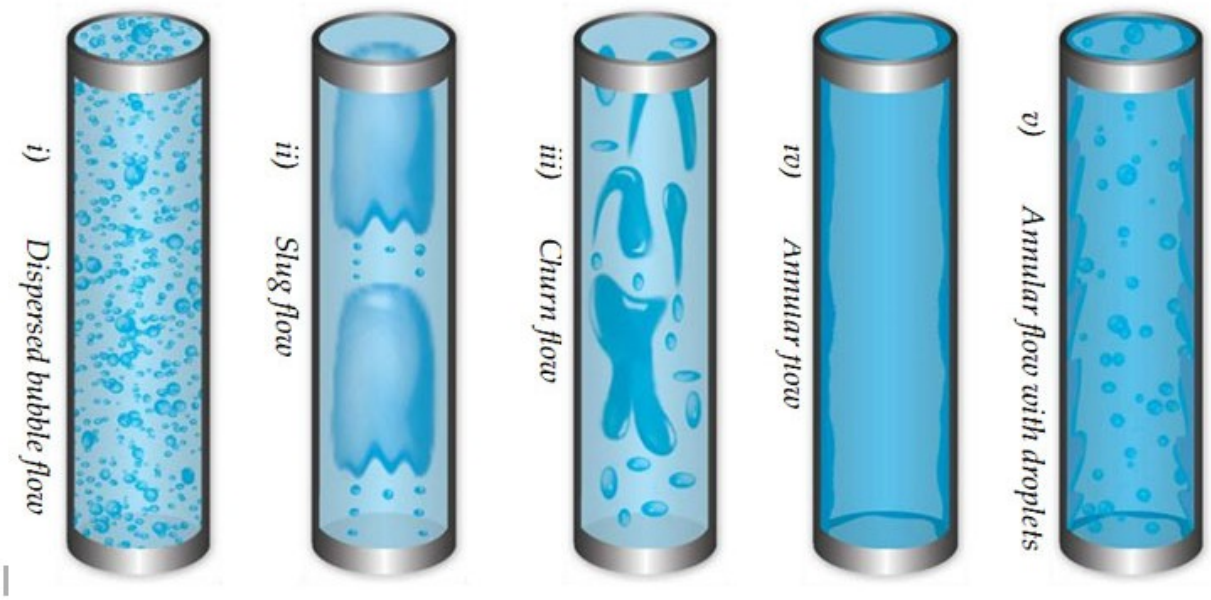

Figure (2.341): Flow patterns in vertical upward flow

2.4 Flow pattern maps

Flow pattern map is one of the most important things to consider in two-phase flow design problems. For some of the simpler flows, such as those in vertical or horizontal pipes, a substantial number of investigations have been conducted to determine the dependence of the flow pattern on component volume fluxes, (J_A, J_B), on volume fraction and on the fluid properties such as density, viscosity, and surface tension. The results are often displayed in the form of a *flow pattern map* that identifies the flow patterns occurring in various parts of a parameter space defined by the component flow rates. The flow rates used may be the volume fluxes, mass fluxes, momentum fluxes, or other similar quantities depending on the investigator. Summaries of these flow pattern studies and the various empirical laws extracted from them are a common feature in reviews of multiphase flow.

One of the basic fluid mechanical problems is that these maps are often dimensional and therefore apply only to the specific pipe sizes and fluids employed by the investigator. A number of investigators (for example Baker 1954, Schicht 1969 or Weisman and Kang 1981) have attempted to find generalized coordinates that would allow the map to cover different fluids and pipes of different sizes. However, such generalizations can only have limited value because several transitions are represented in most flow pattern maps and the corresponding instabilities are governed by different sets of fluid properties. Even for the simplest duct geometries, there exist no universal, dimensionless flow pattern maps that incorporate the full, parametric dependence of the boundaries on the fluid characteristics. Moreover, the implicit

assumption is often made that there exists a unique flow pattern for given fluids with given flow rate.

In summary, there remain many challenges associated with a fundamental understanding of flow patterns in multiphase flow and considerable research is necessary before reliable design tools become available. Figure (2.41) and figure (2.42) depicts how the various flow regimes are represented in a flow pattern maps.

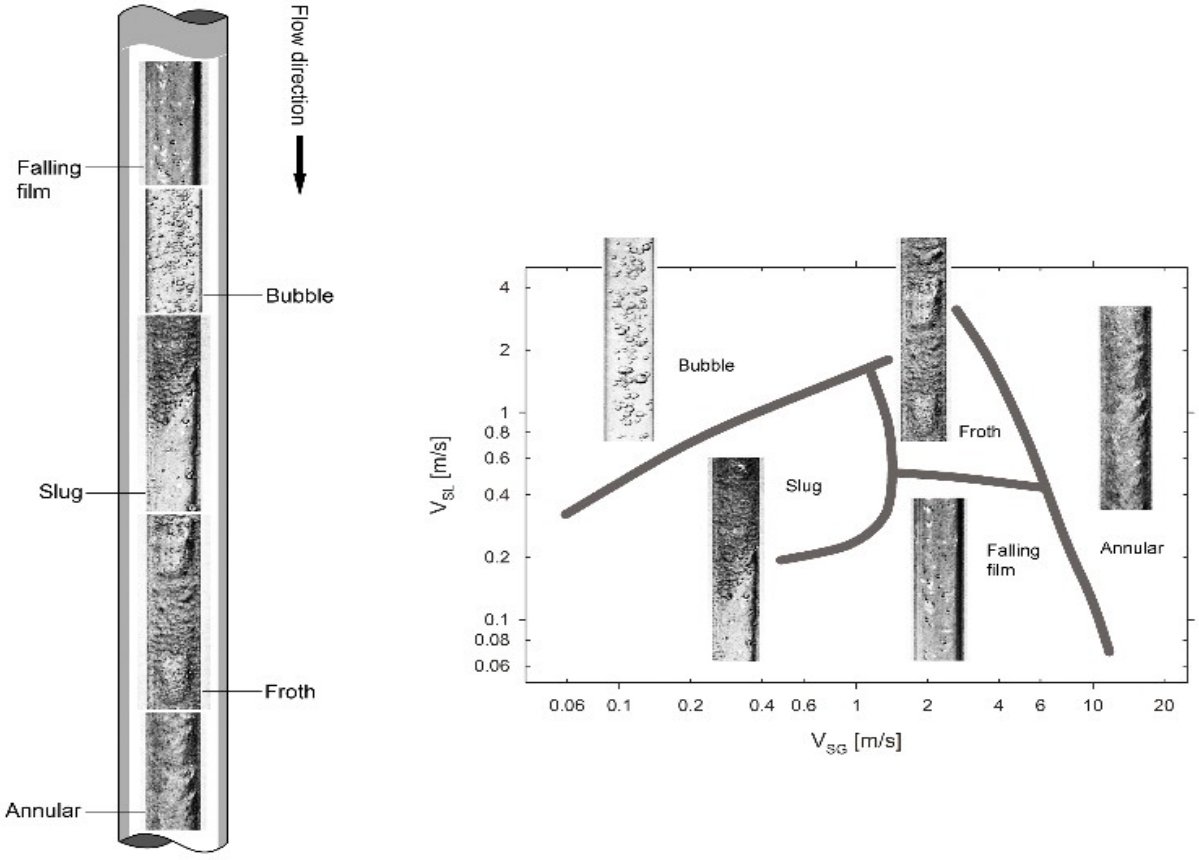

Figure (2.41): Flow Pattern Map showing boundary and transition of flow regime.

(Source: http:// www.google.com/imgres?q=flow+pattern+map&hl)

Figure (2.42): Flow regime map showing the different flow regimes.

Most general two-phase flow correlations and models suffer from a lack of physically-sound flow regime models because characterization of the different hydrodynamic properties is a highly complex task. Therefore, the flow regimes form the bed rock of many of the proposed two-phase flow models. "Parametric relationships are developed, valid for a limited range of flow patterns, to describe the dependence of the predicted/measured flow properties on the consequent flow conditions. It is wholly assumed that the flow regime present is either clearly recognizable or known a priori" **Abdulkadir (2011)**. Figure (2.43) shows the flow evolution as a single phase flow changes to multi-phase flow as the fluid confining pressure is reduced along the flow string.

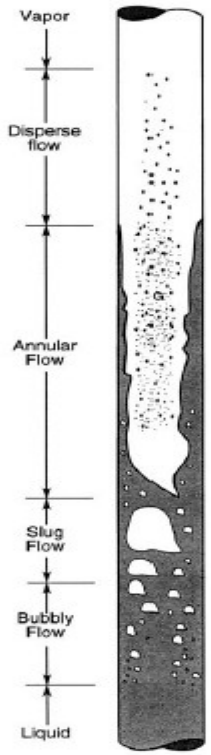

Figure (2.43): Flow evolution of a multiphase fluid along a flow string.
(*authors.library.caltech.edu/25021/1/chap7.pdf*)

2.5 Pressure Drop determination

The fundamental equation for a pressure gradient in a single-phase flow is derived from mass- and momentum conservation equations and is usually stated as (Brill and Mukherjee 1999).

The first, second and third terms in equation (2.51) describe gravitation, friction, and acceleration components of pressure gradients, respectively **(Khasanov et al, 2009).** In a homogenous fluid model, the fluid is characterized by an effective fluid that has suitably average properties of the liquid and gas phases.

The pressure-drop component caused by friction losses requires evaluation of a two-phase friction factor. The pressure drop caused by elevation change depends on the density of the two-phase mixture which is usually calculated with equation (2.52):

Equation (2.53) is used in the case of churn/annular flow, where liquid holdup is replaced by liquid film fraction. The later equation will be used in this work since the consideration is annular flow.

For high velocity churn/annular flow, most of the pressure drop in vertical flow is caused by frictional pressure drop component. This is due mainly to the high shear stress between the fast moving gas core against the liquid film along the pipe body. The pressure-drop component caused by acceleration is normally negligible and is normally neglected in vertical multi-phase flow pressure drop calculations.

Many methods have been developed to predict two-phase, flowing-pressure gradients. They differ in the manner used to calculate pressure drops. Few will be used in this work to test their performance against the experimental data used in this work. They include; Beggs and

Brill, Friedel et al, Poettmann and Carpenter, modified Hagedorn and Brown, Baxendel and Thomas, and Chisholm empirical correlations.

The following chapter will present the experimental facilities, designs procedures employed in deriving the void fraction and total pressure drop data used in the analysis.

CHAPTER THREE

EXPERIMENTAL DESIGN

The main objective of the current study as presented in Chapter 1 is to obtain experimental data for parameters necessary for design such as pressure drop and in two phase flow for vertical pipes with inner diameters similar or close to those typical of oil field applications. Therefore, the two phase flow experiments in this work were carried out on the large scale closed loop facility in the Department of Chemical and Environmental Engineering at Nottingham University. A number of experimental campaigns were performed in this study to measure total pressure drop using different measurement techniques. This is in addition to a visualization campaign using a high speed video camera. The results of each campaign are presented in the following chapters. In all the experimental runs air and water were used as the test fluids at ambient temperature and a pressure of 3 bar (absolute). During the selection of the gas and liquid superficial velocity ranges the attention has been paid to the erosion velocities those for oil and gas production applications. In this chapter, namely in Section 3.1 the major components of the large scaled two phase flow closed loop test facility are outlined, followed by the Sections 3.2 which describe the measurement techniques employed in the present study. The visualization study arrangement and experimental conditions are presented in sections 3.7 and 3.8 respectively.

3.1 Large Scale Two-phase Flow Closed Loop

The large scale closed loop test facility was used previously by Omebere-lyari (2006) in part of his work. A data schematic flow diagram of the rig is shown in Figure 3.1 and the major components of the test facility are illustrated in Figure 3.2.

The test facility consists of an 11 in. riser with 127 mm inner diameter. The water stored in the bottom of the separator is used as the liquid phase and was delivered to the riser base by a centrifugal pump (ABB IEC 60034-1) with a volumetric flow rate up to 68 m^3/hr. The separator is a cylindrical stainless steel vessel of 1 in. in diameter and 4 in. height with a capacity of 1600 liters. The separator is the source of the liquid phase to the system. Therefore, it must be filled partially with water before the start of the experiments. Air was used as the gas phase. The fluid properties used are as shown in Table 3.1. Two liquid ring pumps with 55 kW motors were employed to compress and deliver the air to the riser base. The gas flow rate was regulated by varying the speed of the motors (up to 1500 rpm) and by operating valves VFla and VF3a. The gas and liquid phases come together in the mixing unit at the riser base. The mixing device consisted of 105 mm diameter tube placed at the center of the test section (127 mm). The gas passed up this tube and the liquid phase entered in the annular space between this tube and the test section wall (Figure3.2e).

Downstream of the mixer; the gas and the liquid both travel together through the riser to the measurement section. The measurement device used was pressure tapings. The locations of these techniques are given below:

Two pressure tapping holes were drilled in the test section at 6.69 m and 8.33 m from the mixer (i.e., 52.7 and 65.6 pipe diameters respectively) for measurement of time-varying, pressure difference over 1.64 m (12.9 pipe diameters).

Beyond the riser the two phase flow travels along 2.34 m of horizontal pipe and then 9.6m downward in a vertical pipe before the flow is directed horizontally for 1.47 in to the separator, where the gas and the liquid separated and directed back to the compressors and the pump respectively, so creating the closed loop.

Air from the main supply is used to pressurize the system before the start of the experiments. For the present work the system pressure set at 3 bar. Several valves were used to regulate the flow of the gas and the liquid, namely valves VFla and VF3a for the gas and VF2a and VF4a for the liquid. The liquid and the gas flow rates were monitored using calibrated vortex and turbine meters respectively. The temperature and the pressure of the system were monitored, close to the liquid and the gas flow meters and at the riser base. Before using this facility the operator was made familiar with all the safety features and the operating instructions.

Table (3.1): Properties of the fluids at a pressure of 3 bar (absolute) and at the operating temperature of 20°C

Fluid	Density (kgm^{-3})	Viscosity ($kgm^{-1}s^{-1}$)	Surface tension (Nm^{-1})
Air	3.55	0.000018	
Water	998	0.00089	0.072

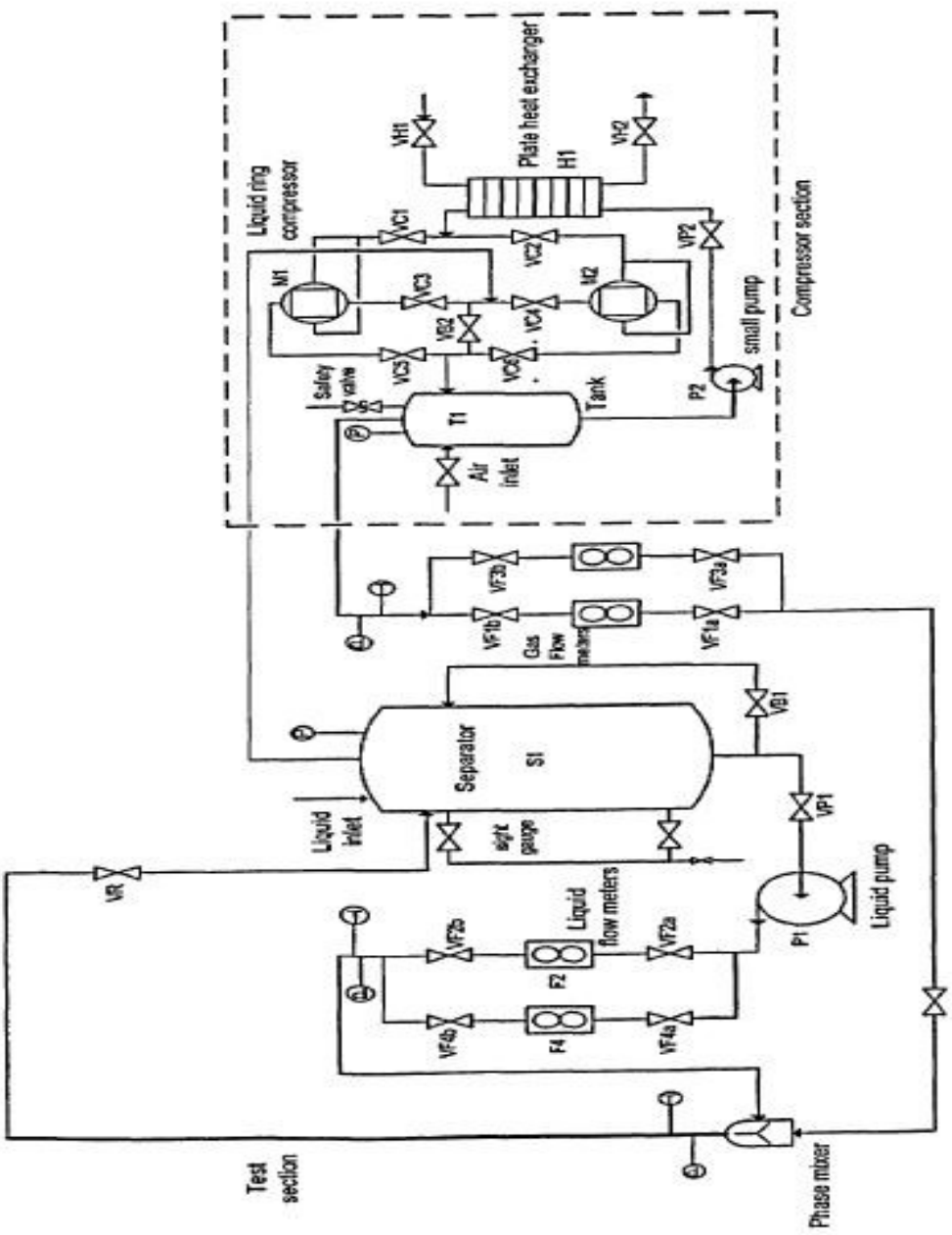

Figure 3.1 Flow sheet of the large scale closed loop facility (127 mm) in the Department of Chemical and Environmental Engineering/Nottingham University

Figure 3.2 The major components of the rig : a) The liquid vacuum pumps b) The liquid centrifugal pump c) The pressure tank d) The separator e) The diagram of the mixing unit and f) The riser.

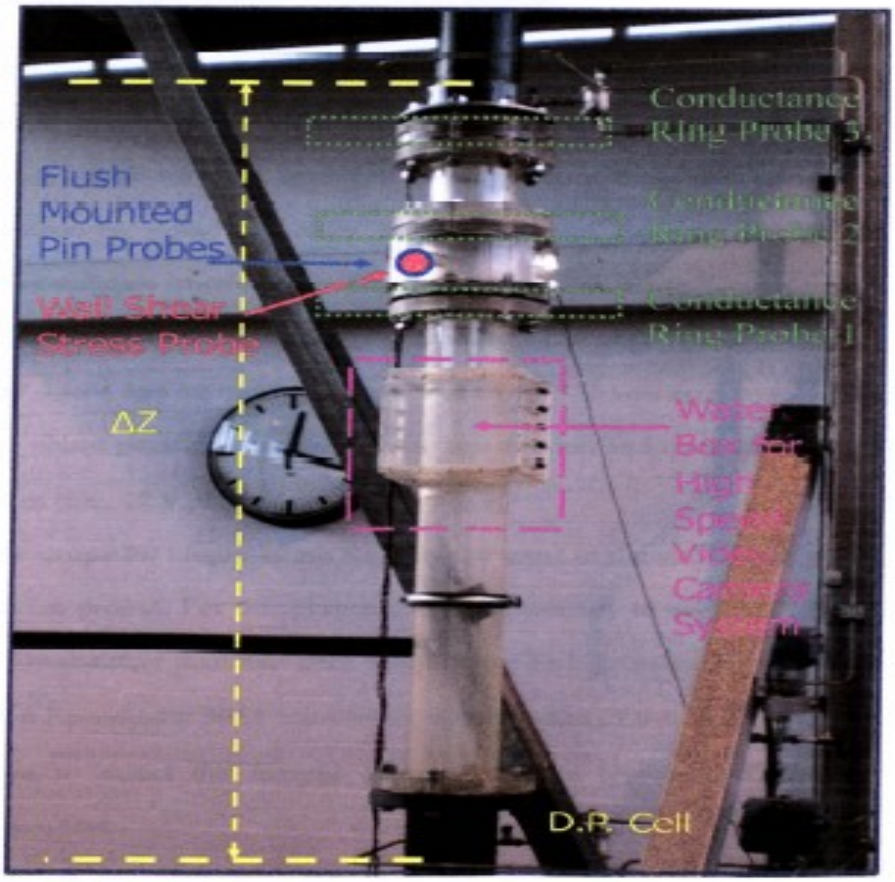

Figure 3.3 The locations of the measurement techniques on the transparent test section of the riser.

3.2 Pressure Drop Measurement

Pressure drop is the driving force for the flow and is therefore an important design parameter. In all the two phase experimental campaigns presented in this study, time-varying, averaged total pressure drop has been measured simultaneously with the other parameters and as a result a bank of experimental data of two phase pressure gradient were obtained. An electronic differential pressure transmitter (Rosemount 1151 smart model) with a range of 0- 37.4 kPa

and an output voltage from 1 to 5V was employed to measure the two phase pressure drop across the test section and over an axial distance of 1.64 m (i. e., 12.9 pipe diameters).

3.3 Visual studies

A high speed video camera (Phantom V7, 1000 fps) has been used to visualize the complex structure of air-water flow in the riser. The images were taken in the transparent section of the test section between 7.65 m and 7.85 m (i. e., 60.2 and 61.8 pipe diameters respectively) from the mixer. To reduce the pipe optical curvature the test section was enclosed with a cubic and transparent box filled with water (Figure 3.3). The picture quality was improved by covering the rear of the pipe with a black plastic sheet as a background and a light source was employed for the clarity of the images. The high speed camera system shown in Figure 3.18.

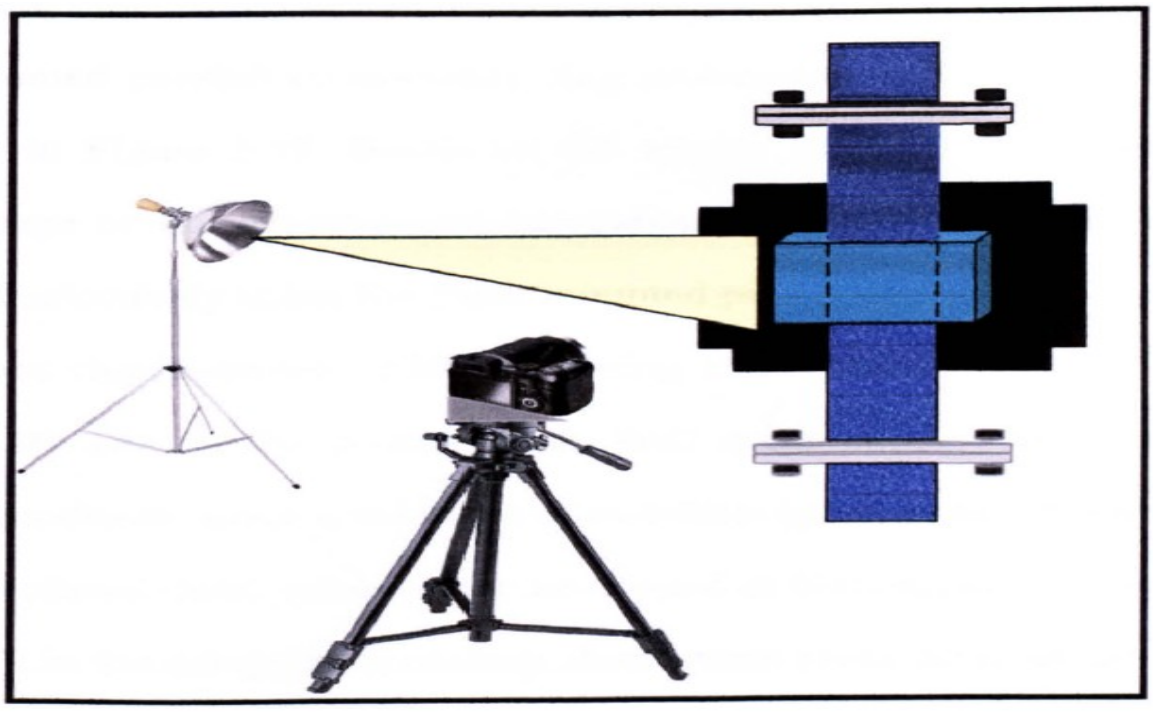

Figure 3.18 High speed video camera systems.

3.4 Experimental conditions

The experiments presented in this study was performed on a large diameter vertical pipe at various gas and liquid superficial velocities ranging from 3.45-16.05 m/s and 0.08-0.2m/s respectively. Experimental data on total pressure drop were obtained in systematically planned campaigns which are summarized below:

In the first stage a total of 119 runs were performed to measure the total time-varying and averaged pressure drop along the riser using a Differential Pressure Transducer (DP cell) at seven (7) different liquid velocities but four of those liquid velocities were chosen for the analysis in this study. The liquid velocities of 0.08-, 0.02-, 0.1-, and 0.2 m/s were selected because it captures an adequate range for a satisfactory pressure drop analysis.

In the experiment, a specific liquid superficial velocity was kept constant and the superficial gas velocity was varied seventeen times. This resulted in changes in geometrical configuration of the fluid flow and hence different pressure drops. the In the experimental analysis, four superficial liquid velocities were chosen; 0.02 m/s, 0.08 m/s, 0.1 m/s and 0.2 m/s. The extremes of 0.02 m/s and 0.2 m/s were chosen in order to capture the total pressure drop at a wider range.

Each liquid superficial velocity corresponds to seventeen (17) superficial gas velocities, and for each of these superficial gas velocity there is a corresponding pressure drop. Nine out of the seventeen average pressure drops that corresponds to each superficial gas velocity at a particular liquid superficial velocity were chosen to get a plot of the time series against the corresponding total pressure drop.

Pressure drop correlations of Friedel (1979), Modified Hagedorn and Brown (1964), Baxendel and Thomas (1961), Poettmann and Carpenter (1952), Beggs and Brill (1973), and Chisholm

(1973) correlations were used to determine the pressure drop using the data from the experiment conducted by Dr. Mukhtar Abdulkadir. The procedure and calculation steps are presented in appendix A.

CHAPTER FOUR

RESULTS AND DISCUSSION

4.1 Introduction

Although pressure drop measurements are very common in two-phase flow due to its importance, there is still a lack of clear experimental data on this parameter in large diameter vertical pipes, i.e., the range of those obtainable in the oil and gas industry. In this study, a data bank of 119 experimental runs were carried out measuring total pressure drop and liquid holdup in a 127 mm diameter pipe for a range of liquid superficial velocities from 0.02m/s to 0.2m/s and the gas superficial velocities from 3.45 m/s to 16.05m/s. The system pressure during experiments was set at 2 bar(g). The frictional pressure drop data was obtained from the measured total pressure drop and the liquid hold up by computing the static pressure loss using equation (4.11) then subtracting the value from the total pressure drop (equation 4.12). Frictional pressure drops for liquid velocities of 0.02 m/s, 0.08 m/s, 0.1 m/s and 0.2 m/s were calculated using the above method based on the data from the experiment.

Due to the lack of experimental data in large diameter pipes it will not surprising if there is no specific correlation derived based on experimental data in such pipe sizes. This being the case, in this Chapter some of the commonly used correlations and models for total pressure drop are examined against experimental data. The data obtained from the experiment were analyzed in different ways and the results are presented in this chapter.

4.2 Time-varying pressure drop

The total pressure drop data in the literature are mainly presented in the form of mean values. This does not always show the additional information available in the time-varying data. Here we present some representative time series of pressure drop to highlight trends in the data. In this study, data on total pressure drop as a function of time were obtained directly from the Differential Pressure transducers (DP cell).

Time-averaged total pressure drop for the ranges 0.02-0.2 m/s of liquid superficial velocity and 3.45-16.05 m/s of gas superficial velocity are presented in the subsequent sections. Firstly, the total pressure drop profile with time are examined, then the effect of liquid and gas superficial velocity on time-averaged total pressure drop for the present work are discussed.

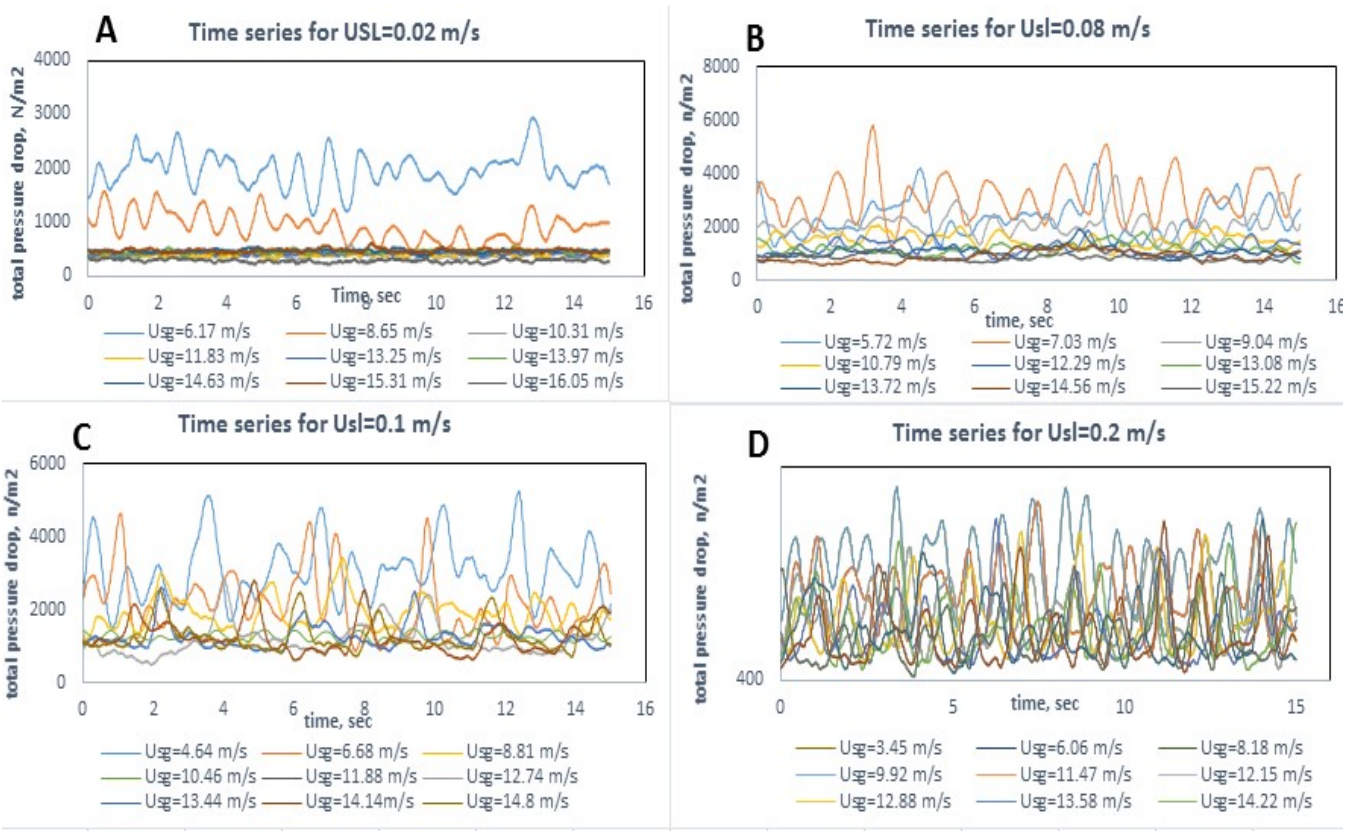

Figure (4.21): A plot of total pressure drop at different gas and liquid velocities against time.

From Figure (4.21 **A**), it can be observed that the gas superficial velocity of 16.05 m/s has the lowest pressure drop followed by the lower values. The pressure drop for gas superficial velocities of 6.17 and 8.65 m/s vary in a sinusoidal manner with time and distance along the pipe wall. This could be attributed to the presence of waves on the liquid film. When the waves are no longer present, the pressure drop for gas velocities of 10.31-, 11.83-, 13.25-, 13.97-, 14.63-, 15.31-, and 16.05 m/s are fairly constant with time and distance along the pipe length. Thus, at a higher gas velocity the pressure drop stabilizes with time.

It can be observed from Figure (4.21 **B**) that at the highest gas superficial velocity, Usg of 15.22 m/s, the lowest pressure drop is seen and the profile again is sinusoidal. It can be

observed from the plot that as the gas superficial velocity increases the total pressure drop approaches a constant value.

From Figure (4.21 **C**), the variation in total pressure drop with time also increases with decrease in gas superficial velocity, with the lower values of gas superficial velocities having a more erratic profile than the higher ones. The erratic behavior can be explained in terms of the prevailing flow pattern, which in this case is churn flow.

On the other hand, Figure (4.21 **D**) depicts the behavior of total pressure drop with time for the different gas superficial velocities investigated. The results show that the trend is fairly uniform except for the lower values of gas superficial velocities which is more erratic than others.

It can be concluded therefore that:

- Total pressure drop increases with increase in liquid superficial velocity for a constant gas velocity.
- As the gas superficial velocity increases at constant liquid superficial velocity, the total pressure drop profile becomes less erratic (approaches a constant value) with time along the pipe length. In other words, the extent of fluctuation in the pressure drop grows as the gas flow-rates are reduced as a consequence of a change in flow pattern from annular to churn flow.
- The variation in total pressure drop with time increases as liquid superficial velocity increases for a constant velocity. This can be seen more clearly in Figure (4.23).

This fluctuating nature in the time series of total pressure drop has been linked to the characteristic of flow patterns by some researchers, for instance Hernandez-Perez (2008) has

attributed that to the occurrence of slugs. From similar perspective the fluctuation observed in the time series of total pressure drop in the present study especially for low liquid flow rate can be linked to the transition from churn to churn-annular or annular flow regime as the variation of total pressure drop with time becomes less disturbed as the gas superficial velocity rises to a certain value.

According to Hernandez-Perez et al (2010) the unsteady character in the time varying total pressure drop can lead to the conclusion that the average value of pressure drop might not be accurate enough for design purposes as the critical pressure drop can get bigger than that and instead the standard deviation in the relative form can be used which is taking the size of the fluctuations into account with respect to the mean value of the pressure drop. (**Zangana 2011**)

4.3 The effect of liquid and gas superficial velocities on the total pressure drop.

The effect of liquid flow rate variations on time-averaged total pressure drop based on the experimental data is shown in Figure (4.30).

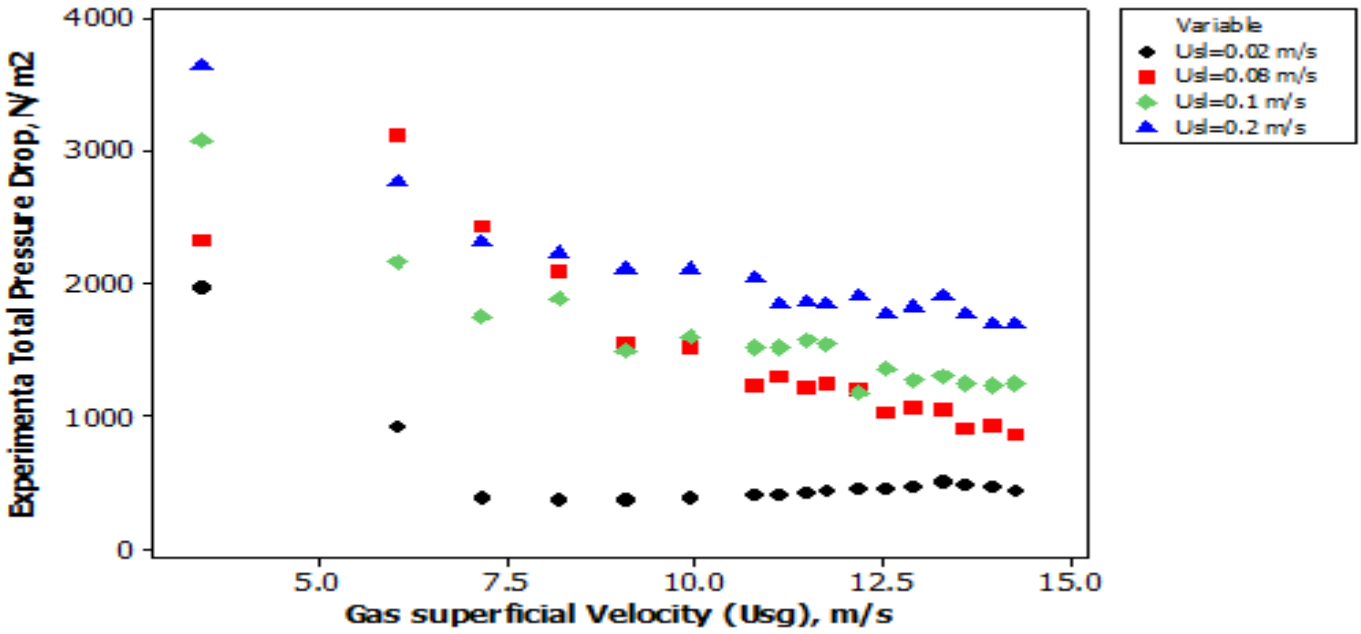

Figure (4.30): Total pressure drop as a function of gas superficial velocity

The general trend of the graph is that the time-averaged total pressure drop decreases systematically as the gas flow rate increases. This might be explained based on the fact that the flow is gravity dominated, i.e., the major contributor to total pressure drop in a vertical pipe is static pressure drop. This indicates that the lower the gas superficial velocity the higher the total pressure drop. It can also be noticed that the total pressure drop increases with liquid velocity. However, the change in pressure drop with liquid superficial velocity is more pronounced between liquid velocities between 0.02-0.08 m/s. A better explanation which was provided by Holt (1996) is that most of the liquid flow rate is in the form of entrained droplets

and that any further increase in it will only serve to increase the entrained liquid flow rate. As a result the film flow rate and the film thickness will not change significantly and hence the limited influence of the liquid flow rate on the two-phase total pressure drop. The effect of the liquid film fraction on the total pressure drop is depicted in Figure (4.33).

It can be seen that over the range of gas superficial velocities studied, two major regions of total pressure drop can be identified as a result of gas flow rate variations; the first area being at low gas velocities between 3.45-9.42m/s, where the total pressure rapidly drops as the gas superficial velocity increases before the trend is changed to a gradual decrease in the total pressure drop at higher gas superficial velocities. It is suggested that the change of the slope linked to a transition of flow regime from churn to annular flow.

It can be concluded therefore that the liquid and gas superficial velocities has a significant effect on the total pressure drop.

The effect of liquid and gas flow rate on total pressure drop can also be presented by plotting the total pressure drop as function of mixture superficial velocities (U_{sg}+ U_{sl}) as shown in Figure (4.41) or gas mass flux ($\rho_g.U_{sg}$). Similar forms are reported by researchers, e. g., Kaji et al (2007), Kaji and Azzopardi (2010), Sawai et al (2004), Holt (1996), and Govan (1990). It is worth mentioning that in using gas mass flux the effect of gas density is taken into account. However the differences in the plots for the present work will not change significantly from what have been discussed earlier and this can be justified based on the fact that Usl << Usg and ρl remained constant for the data presented. Therefore using mixture velocity or gas mass flux terms instead of gas superficial velocity will not change the trend of the graph significantly. However they can remain as a very useful alternative form to present such experimental data.

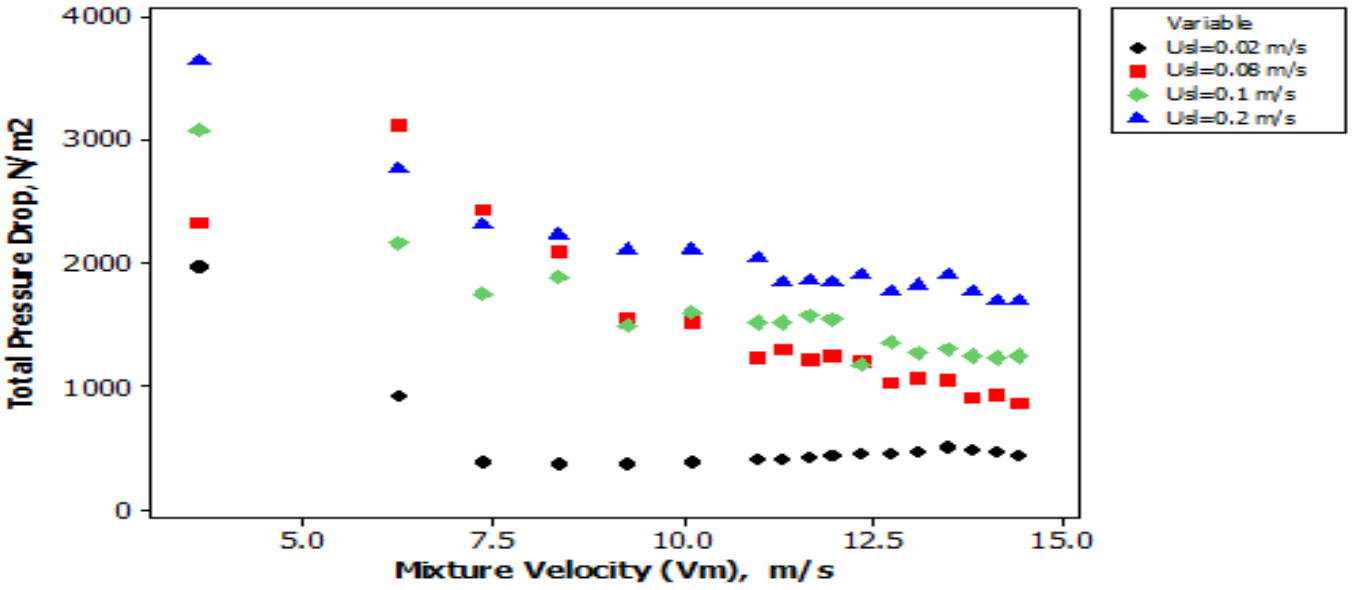

Figure (4.31): Total pressure drop as a function of mixture superficial velocities.

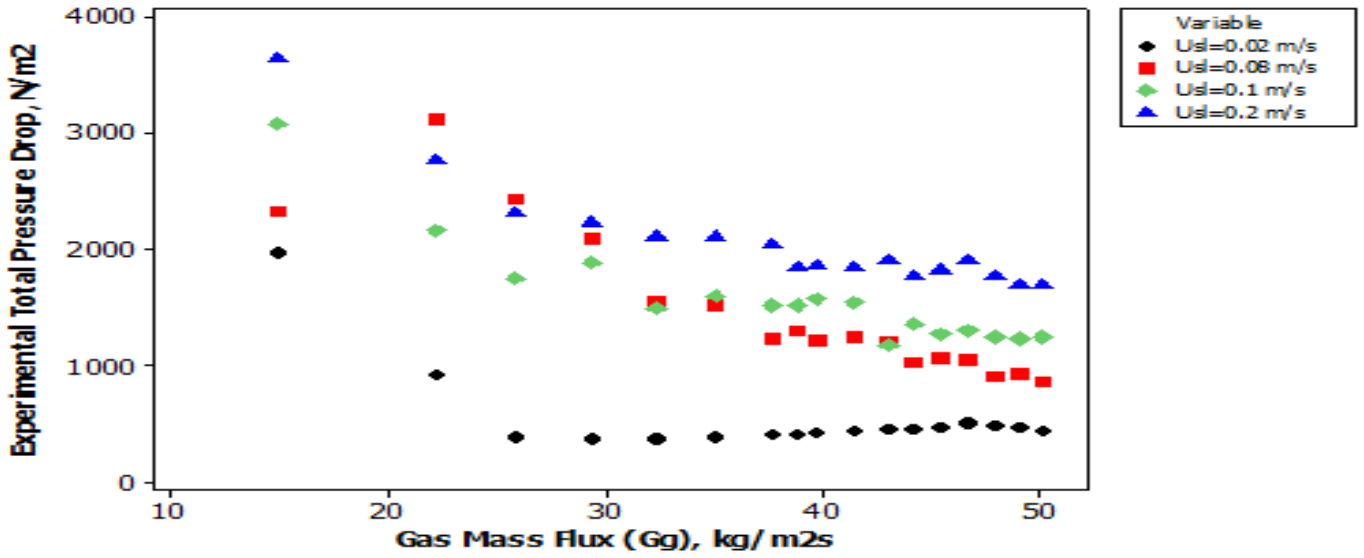

Figure (4.32): Total pressure drop as a function of gas mass flux (G_g).

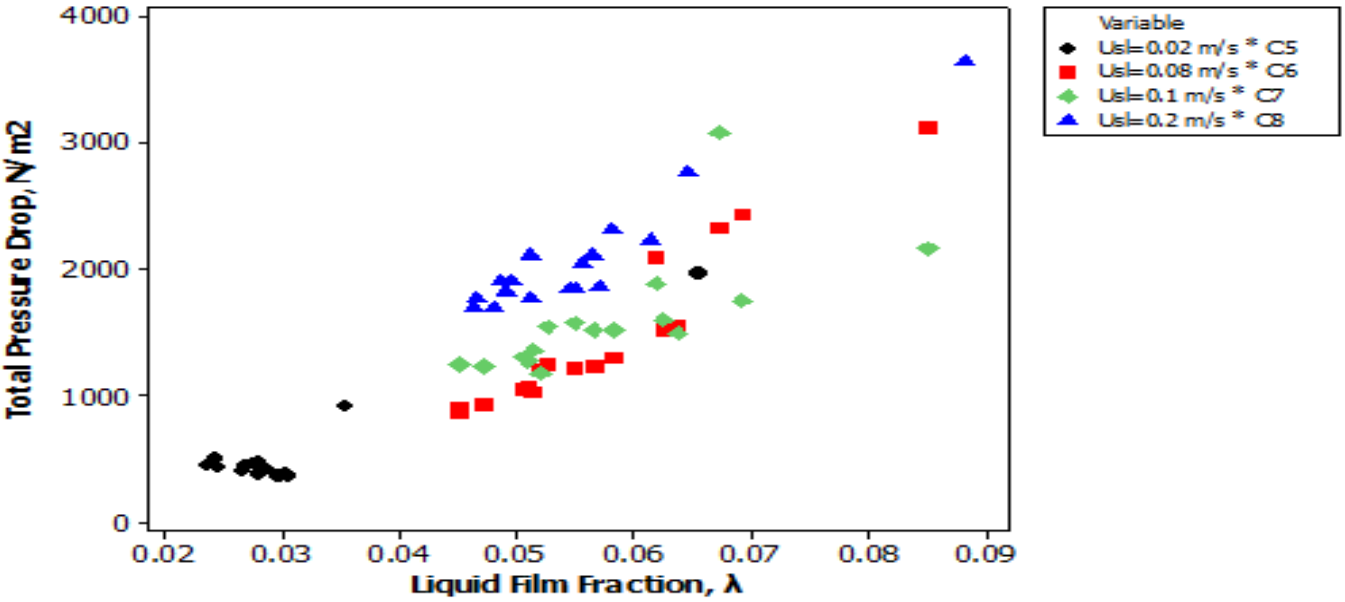

Figure (4.33): Pressure drop as a function of liquid film fraction.

The total pressure drop is related strongly to the liquid film properties such as the shear stress on the pipe wall and on the interface between the gas and the liquid phase this is in addition to the thickness of the film. As can be seen from Figure (4.33), the total pressure drop generally increases with increasing liquid film fraction but at a liquid superficial velocity of 0.02 m/s, the total pressure drop was almost constant except for the last value. It can also be observed that the maximum pressure drop was encountered at the highest liquid superficial velocity. The reason for this might not be unconnected with the very high liquid density which resulted in a higher mixture density.

4.4 Measured frictional pressure drop.

What is noticeable in Figure (4.40) is that the frictional pressure drop for liquid superficial velocity of 0.02 m/s is fluctuating between negative and positive values, this was an unexpected behavior especially for high gas superficial velocities. At such condition, the liquid film is expected to become unidirectional and flow upward on the wall of the pipe according to the typical definition of annular flow in vertical pipe by researchers, e.g., Azzopardi (2006), and Hewitt and Taylor (1970).

The Kutateladze number (K_{ug}) which is given by equation (4.41).

The average Kutateladze number for liquid superficial velocity of 0.02 m/s and gas superficial velocity from 6.17 m/s to 16.05 m/s is 4.615. This is greater than the usually quoted transition value of 3.1 and accordingly the annular flow pattern was expected.

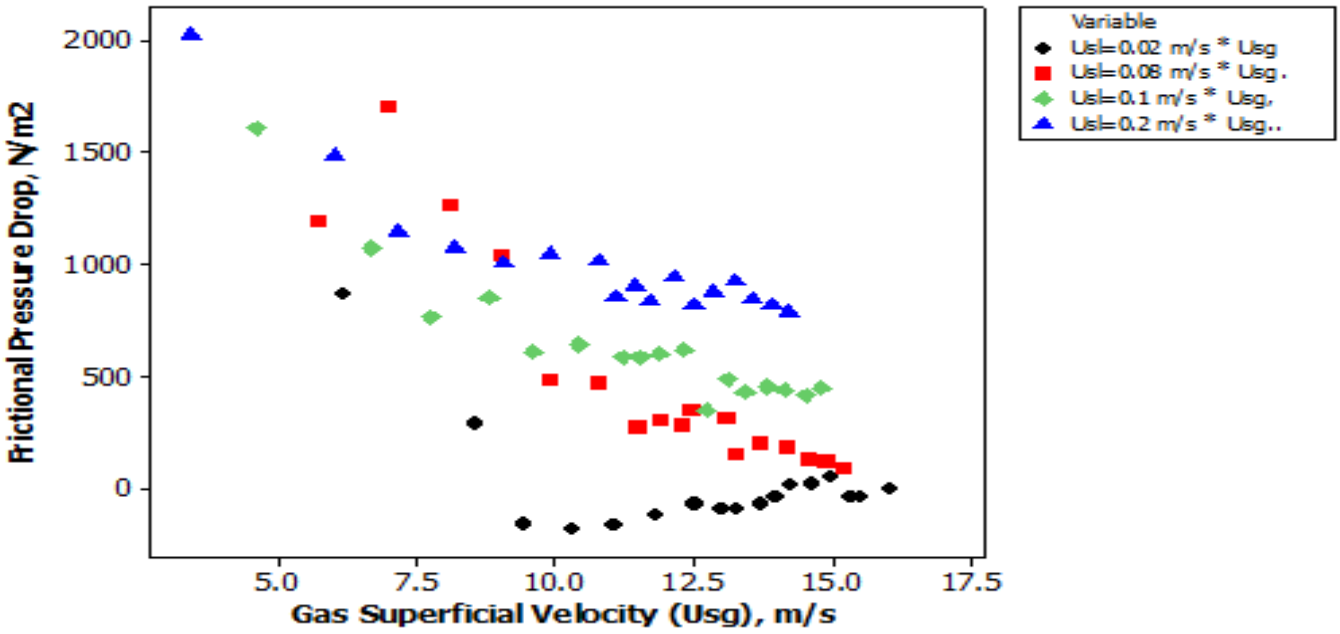

Figure (4.40): Measured frictional pressure drop as a function of gas superficial velocity.

However the behavior of frictional pressure drop mentioned above and illustrated in Figure (4.40), lead to an alternative explanation that the direction of the flow still changing. That is, the flow pattern is affected by the diameter of the pipe. Therefore, the Kutateladze number might not be suitable to indicate the churn-annular transition in such diameter pipe, as it does not contain pipe diameter.

4.5 sensitivity analysis on the effect of diameter on the frictional pressure drop

As stated earlier almost all the available empirical correlations and mechanistic models were developed with small diameter pipes due to lack of data on large diameter pipes. This is a major limitation to the universality of its usage to predicting multi-phase pressure drop. Another limitation is the range of data and the conditions at which these correlations were developed. The frictional pressure drop from the experiment data used in this work were under-predicted by all the models. The reason is not farfetched. The range of data at which the correlations used in this work were developed falls between 1” to 1.5”, which 3.33 to 5 times less than the diameter used in carrying out the experiment for this work (5” or 0.127 m). This analysis were carried out for gas velocity of 0.02 m/s and liquid velocity from 6.17 m/s to 16.05 m/s.

Figures (4.80) through to Figure (4.85) show clearly the effect of pipe diameter on the frictional pressure drop. Pipe diameters of 0.127 m (5”- experimental condition), 0.1016 (4”), 0.0762 (3”) and 0.0381 m (1.5”) were chosen to carry out this sensitivity analysis.

It is clear from the plots that the frictional pressure drop increases with a decrease in pipe diameter. This phenomenon is due to effect of pipe diameter on the Reynolds number which is a function of friction factor. A large pipe diameter increases the Reynolds number which in turn reduces the friction factor. The friction factor is directly proportional to the frictional pressure drop. Furthermore a lower pipe diameter imposes a higher wall shear stress between the gas core and liquid film and between the film and the pipe wall which impedes flow and hence causes large pressure drop.

Also from the plots it can be observed that the change in frictional pressure drop with pipe diameter is largest between diameters of 0.0762 m (3") to 0.0381 m (1.5"). This gives an indication on how pipe diameter affects frictional pressure drop.

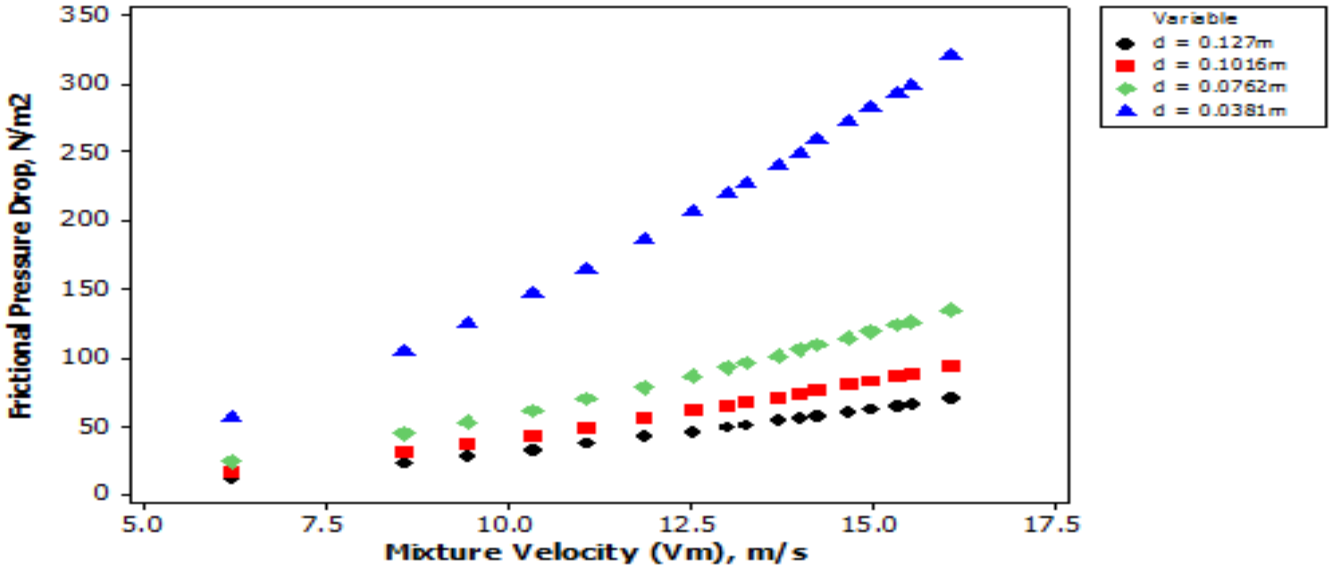

Figure 4.50: Effect of pipe diameter on frictional pressure drop for Friedel (1979) correlation.

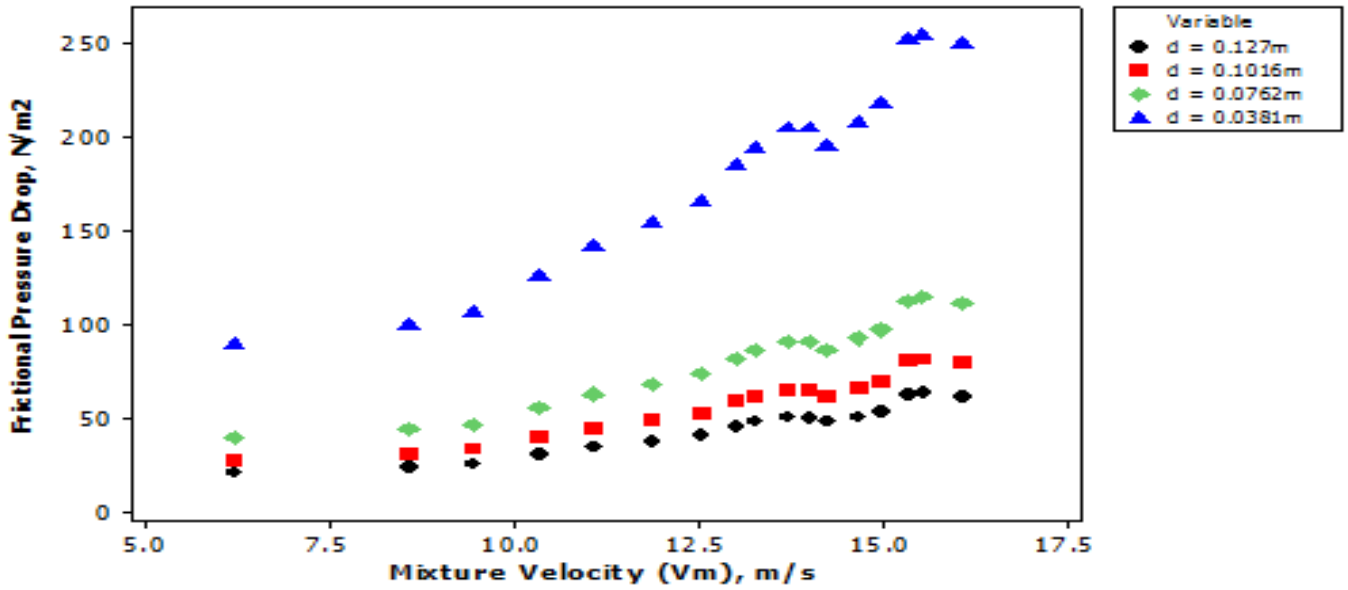

Figure 4.51: Effect of pipe diameter on frictional pressure drop for Beggs and Brill (1973) correlation.

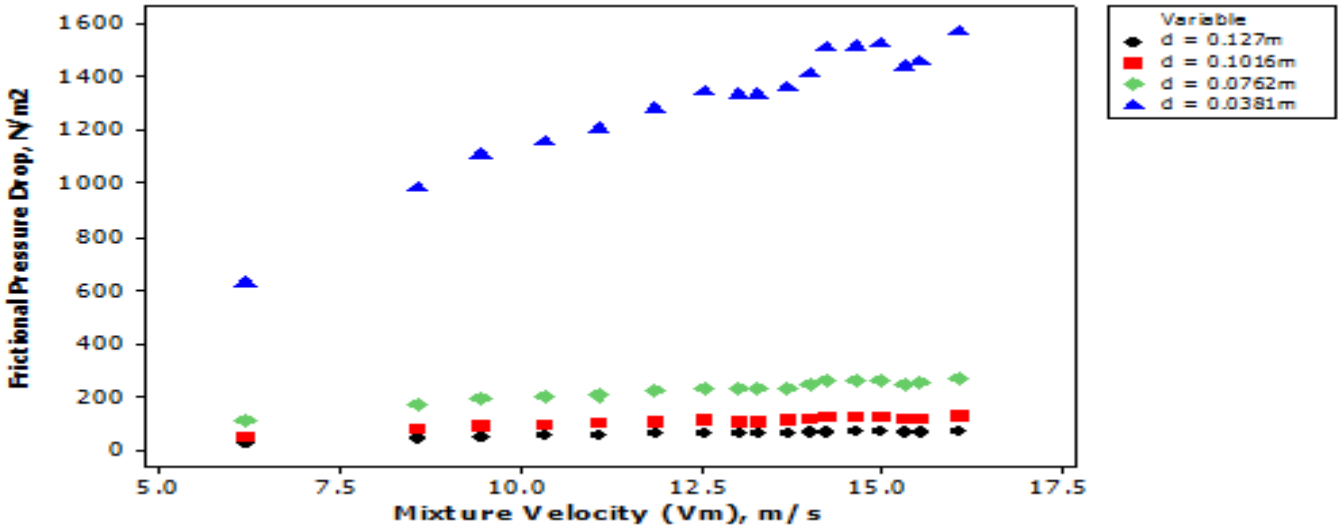

Figure 4.52: Effect of pipe diameter on frictional pressure drop for Poettmann and Carpenter (1952) correlation.

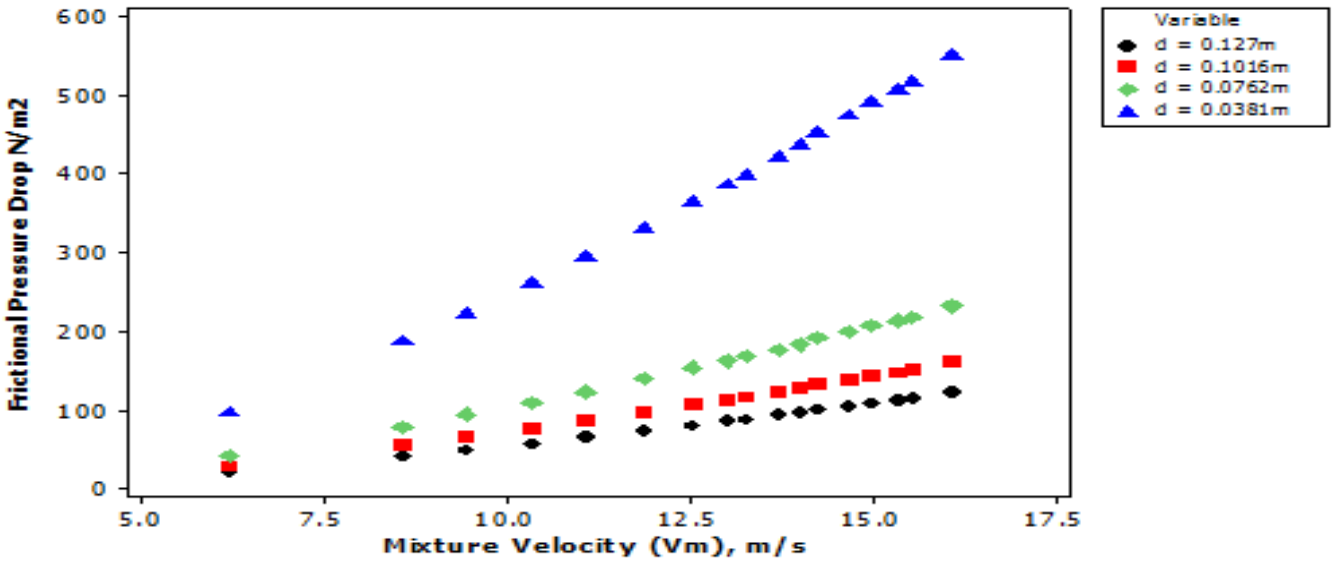

Figure 4.53: Effect of pipe diameter on frictional pressure drop for Chisholm (1973) correlation.

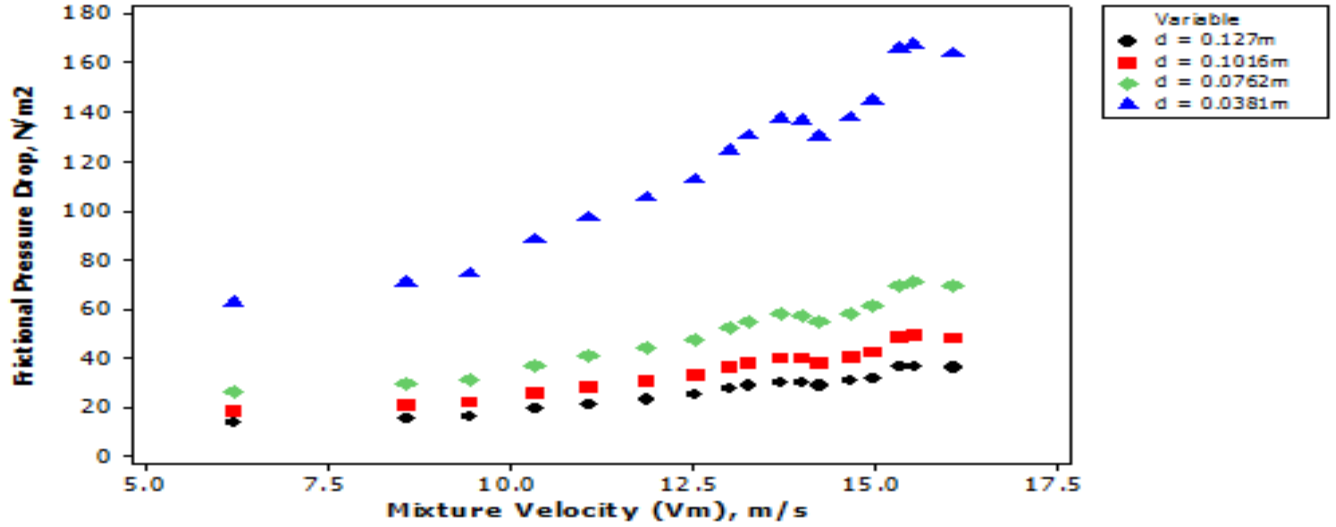

Figure 4.54: Effect of pipe diameter on frictional pressure drop for Modified Hagedorn and Brown (1964) correlation.

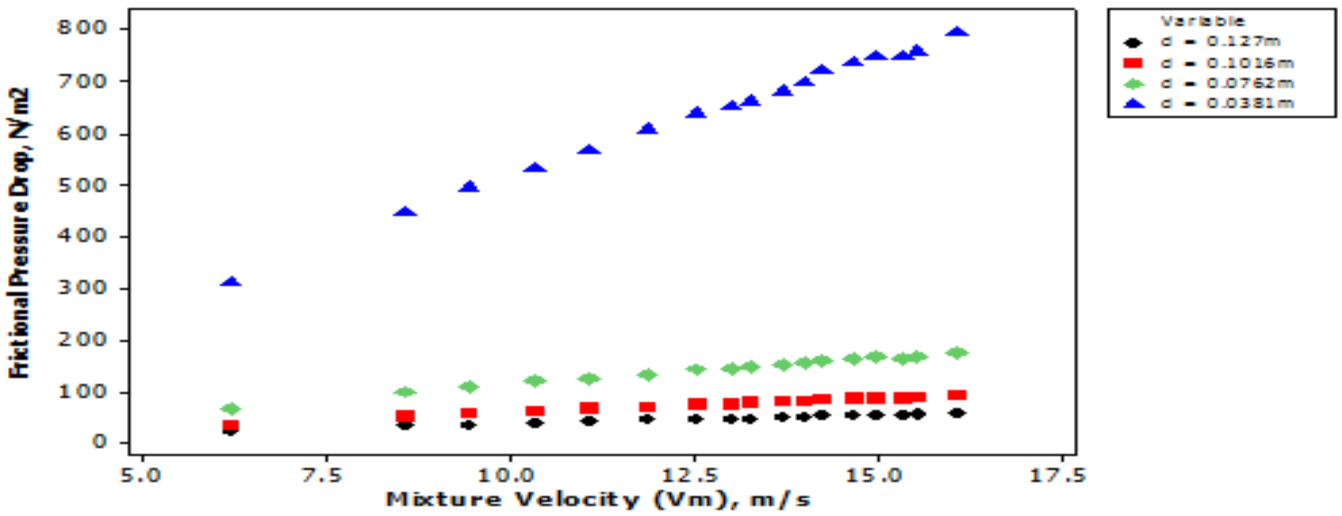

Figure 4.55: Effect of pipe diameter on frictional pressure drop for Baxendel and Thomas (1961) correlation.

From the above analysis, it can be concluded that the empirical correlations used in this work are not good enough to predict frictional pressure drop in a large diameter pipe used in this work. Lists of the known works on the topic can be found in the literature, e. g., Spedding et al (1998), Kaji and Azzopardi (2010), who reported a noticeable effect of pipe diameter on two-phase pressure drop in the range of small diameter pipes, i.e., up to 50 mm. This being the case comparison between present work and the data from different sources in literature and for different diameter pipes can provide very useful information on the flow behavior as the effect of such diameter pipes.

4.6 Comparison between measured and calculated frictional pressure drop.

There are two components of total pressure drop in vertical multi-phase flow, namely the frictional pressure drop and the hydrostatic pressure drop. The hydrostatic component of the experimental pressure drop was calculated using the mixture densities of the experimental fluids (air and water). The calculated hydrostatic pressure drop was subtracted from the total pressure drop to obtain the frictional pressure drop.

There is an unsavory trend in the frictional pressure drop of the experimental data. The values of the experimental frictional pressure drop is decreasing with an increase in void fraction (or decrease in film fraction). This is a highly unexpected behavior because as flow evolves along the flow string gas increasingly occupies the pipe area more than the liquid thereby contributing more to the shear stress and hence frictional drop.

There is an explanation to this unexpected behavior. It could certainly be that most of the liquid film fraction is over-estimated. This is as a result of an assumption in the experimental data that the sum of the void fraction and liquid film fraction is equal to unity. During annular flow regime this assumption can lead to a considerable error in pressure drop prediction. The entrainment of this liquid fraction increase as the gas and liquid superficial velocity increases. This is because a portion of the liquid is entrained as droplets in the central gas core due to turbulence. This liquid fraction does not contribute to the frictional pressure drop. This lead to an under-estimation of the frictional pressure drop and the degree of under-estimation increases as flow evolves. This made the experimental frictional drop and the calculated ones incompatible for an effective comparison, though the values of the calculated frictional pressure drops falls short of the measured values regardless.

4.7 Comparison of experimental total pressure drop with results from empirical correlations.

Several empirical correlations on two-phase gas and liquid flow was investigated to check their performance and validity in characterizing frictional, and hence total pressure drop for the conditions studied in this work (for large diameter air-water flow in a vertical pipe). There has been little experimental data on multi-phase pressure drop in vertical pipe, hence there is no known correlation on this subject on large diameter pipes (>100 mm). The empirical correlations in literature are mainly based on small diameter pipes and this puts a limitation on their usage to characterize multi-phase flow in pipes diameters in the range of those commonly used in the oil and gas industry.

The motive of this work is to compare the pressure drop derived from those empirical correlations to the actual pressure drop from experimental study. This would give us an idea on how each of these empirical correlations perform as compared to the actual results, and more importantly it would give us an information on the effect of pipe diameter on the pressure drop.

The correlations chosen for this study include; Friedel et al (1979), Beggs and Brill (1973), Poettmann and Carpenter (1952), Chisholm (1973), Modified Hagedorn and Brown (1964) and then Baxendel and Thomas (1961) correlations. Each of these correlations were used to calculate the pressure drop using the same set of data derived from the experimental study. The calculation steps and excel model are provided in appendix A.

Table (4.1) show the results of the pressure drop of selected empirical correlations against the results of the pressure drops calculated from six different empirical correlations. The pressure

drop values were derived from a liquid superficial velocity of 0.02 m/s and gas superficial velocity ranging from 6.17 m/s to 16.05 m/s.

Measured ΔP_T	Calculated Total Pressure Drop					
Experimental Result	Friedel et al	Beggs & Brill	Poettmann & Carpenter	Chisholm	Modified Hagedorn & Brown	Baxendel & Thomas
1969.06	1114.22	1123.42	1131.07	1123.43	1115.85	1124.37
918.41	646.64	647.92	669.67	664.85	639.19	656.06
385.73	569.52	567.97	593.96	591.29	558.51	578.01
366.11	577.44	576.23	599.18	602.84	564.64	583.96
371.01	568.87	567.17	588.84	597.42	553.95	573.61
385.73	546.43	543.18	565.12	578.43	528.52	549.20
419.08	530.05	525.35	547.32	565.16	509.32	530.85
420.06	556.90	554.06	570.70	593.96	535.97	555.85
422.03	566.64	564.52	578.76	604.87	545.34	564.53
440.67	564.76	562.39	575.20	604.94	541.98	561.09
449.49	541.31	536.75	552.04	582.93	516.28	536.82
449.69	495.37	486.34	508.44	538.35	466.80	490.52
465.19	503.07	494.32	513.75	547.91	473.33	496.46
503.45	510.24	501.87	518.86	556.58	479.62	502.16
475.00	571.60	569.48	574.12	619.24	543.54	561.20
469.60	566.66	563.95	568.57	615.22	537.57	555.48
443.61	520.05	511.59	522.65	571.45	485.52	506.98

Table (4.1): Comparison of calculated total pressure drop with experimental results.

4.71 Cross plot comparison

Cross plots were used to compare the performance of all the selected models. A 45° straight line between the calculated pressure drop values versus measured pressure drop values is plotted which represents a perfect correlation line. When the values go closer to the line, it indicates better agreement between the measured and the estimated values. When the values are well above or below the 45° line, it indicates over-prediction and under-prediction respectively

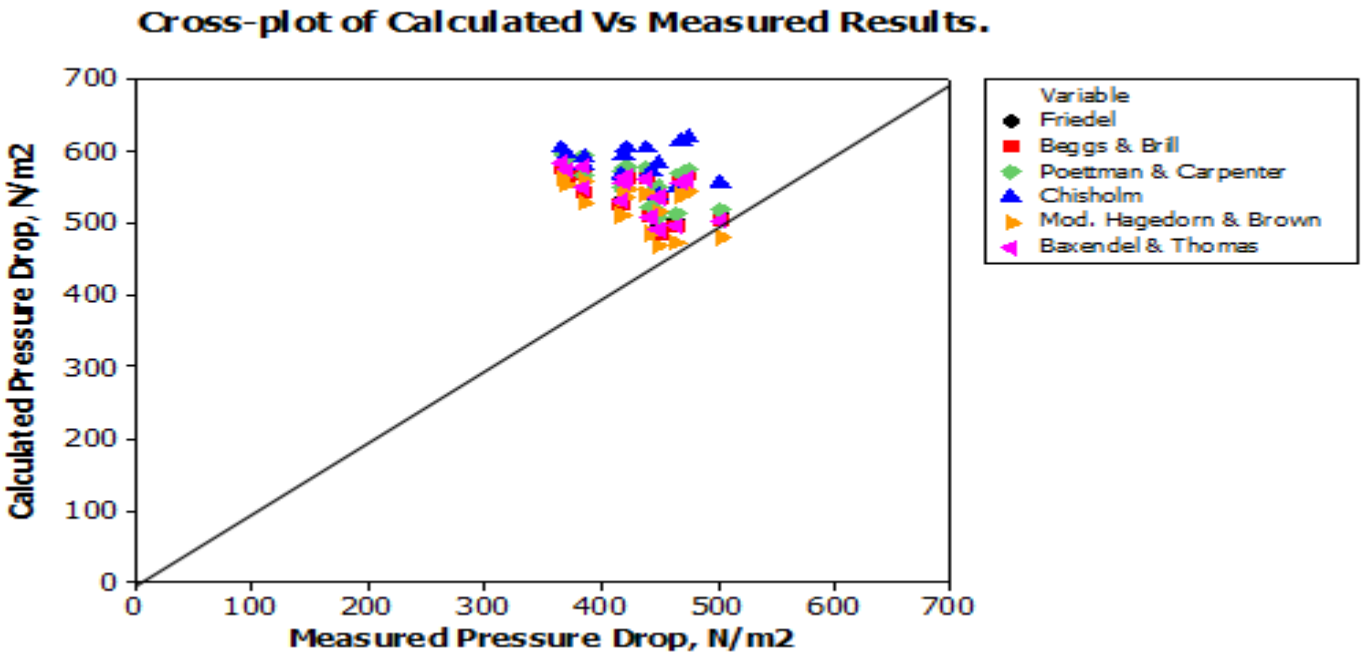

Figure (4.711): Cross plot of pressure drop for all the selected correlations.

Figure (4.711) present cross-plots of estimated pressure drop versus measured pressure drop for all the investigated methods. It has been noticed that all the six methods presented over-estimated the pressure drop by some degree but some are closer to experimental value than others.

The common obstacle for using a pressure drop method whether it is an empirical correlation, a mechanistic model or an artificial neural network model is that most of these models are applicable for specific range of data and conditions in order to predict the pressured drop accurately. However, in some cases, it can work well also in some actual filed data with acceptable prediction error. (**Musaab and Mohammed, 2007**)

To analyze and compare the effectiveness of each correlation or model, the values of both measured and predicted pressure drop are recorded. All the selected correlations and models are evaluated using actual filed data where the predicted pressure drop is compared to the measured one.

It is worthy to mention that there are still many empirical correlations and mechanistic models in the literature which have not been evaluated in this study and may have more or less accurate results when predicting pressure drop in vertical wells. However, the methods were selected based on the authors' perspective. Therefore, all the conclusions and recommendations were based on the selected methods.

4.8 Regression analysis using minitab-16 statistical software

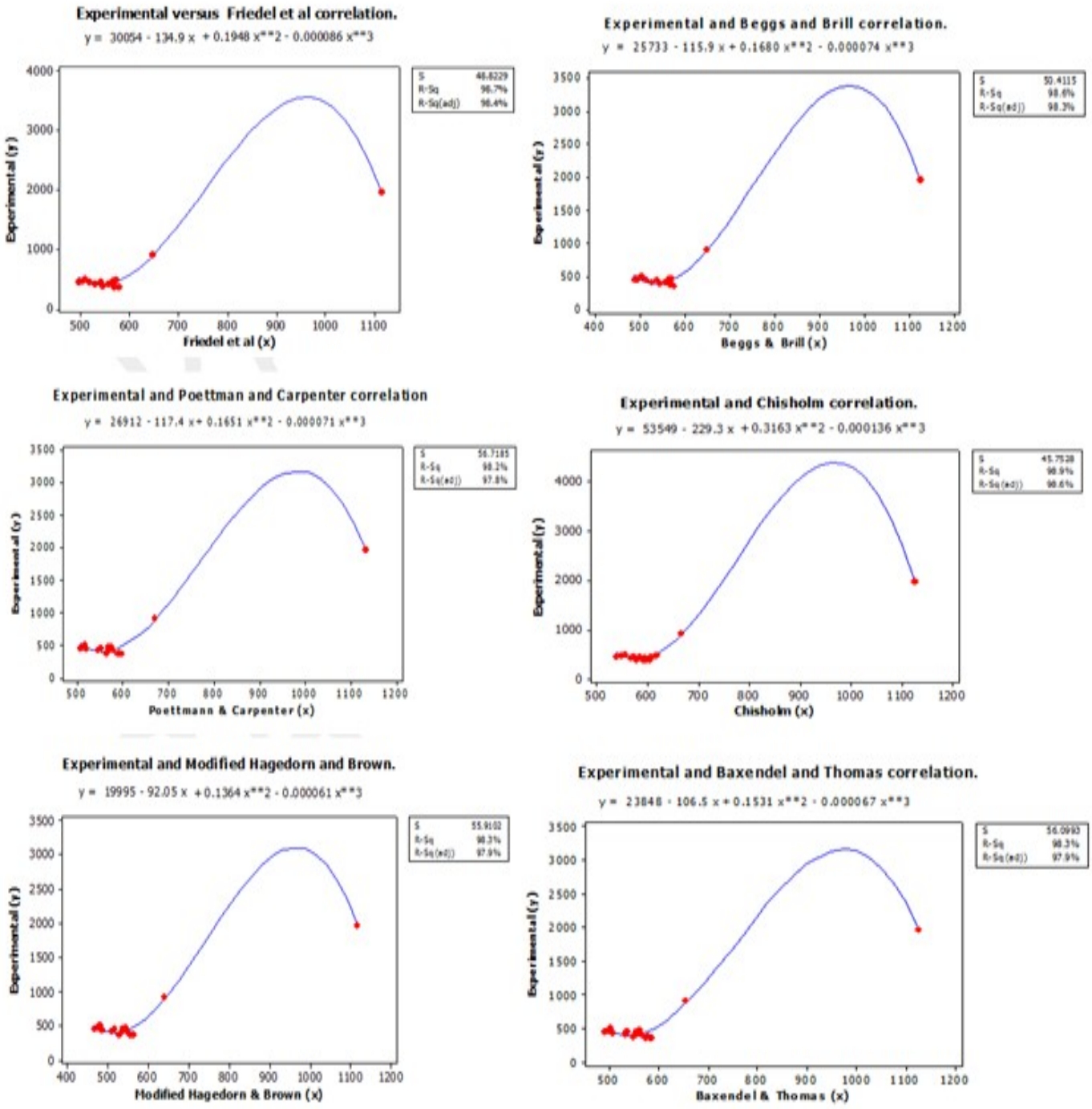

Figure (4.81): Regression analysis of experimental and calculated results.

Cubic regression was chosen as against linear or quadratic regression because it better captures the relationship between the experimental results and that of the various empirical correlations.

Figure 4.82 depicts side by side the closeness or otherwise of the results of the various empirical correlation to the experimental results.

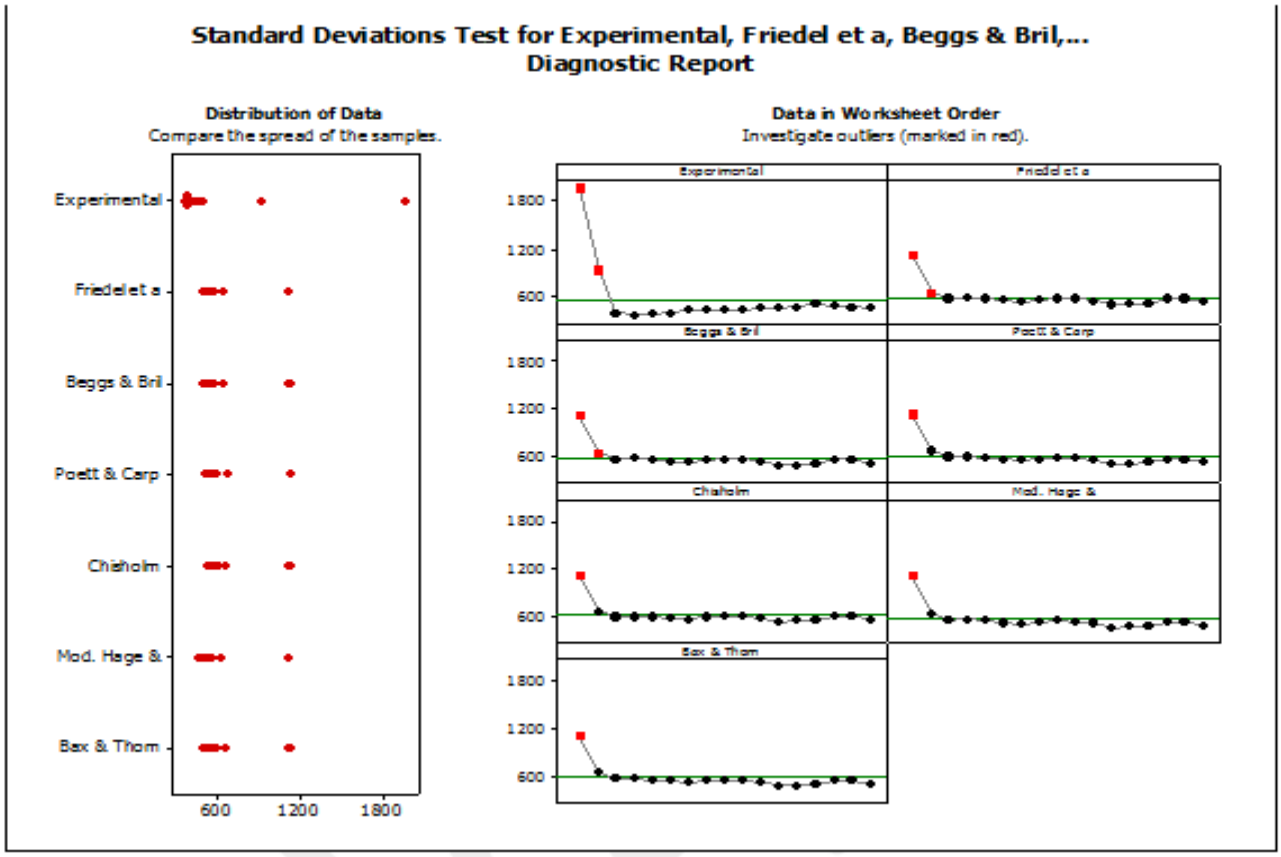

Figure (4.82): Diagnostic report of measured and calculated results.

From Figure (4.96) it can be seen that the results from the empirical correlations follows a similar trend to the experimental total pressure drop results. All the correlations slightly over-predict the total pressure drop with the results of Chisholm (1973) having the highest over-prediction with a mean pressure drop of 621.11 N/m^2 as compared to the mean pressure drop of 550.23 N/m^2 for the experimental result. The modified Hagedorn and Brown (1964) came closest to the experimental result with a mean pressure drop of 564.47 N/m^2. This can be seen more clearly in Figure (4.97).

Standard Deviations Test for Experimental, Friedel et a, Beggs & Bril,...
Descriptive Statistics Report

Sample	Statistics Sample Size	Mean	Standard Deviation
Experimental Result	17	550.23	386.05
Friedel et al	17	585.28	140.86
Beggs & Bril	17	582.15	144.67
Poettmann and Carpenter	17	598.72	142.59
Chisholm	17	621.11	132.89
Modified Hagedorn and Brown	17	564.47	148.01
Baxendel and Thomas	17	583.95	144.84

Table (4.2): Descriptive statistics report of measured and calculated results.

Figure (4.84) mirrors the comparison of the experimental result as against the results of the six empirical correlations chosen for this work. All the correlations followed the same trend as the experimental results.

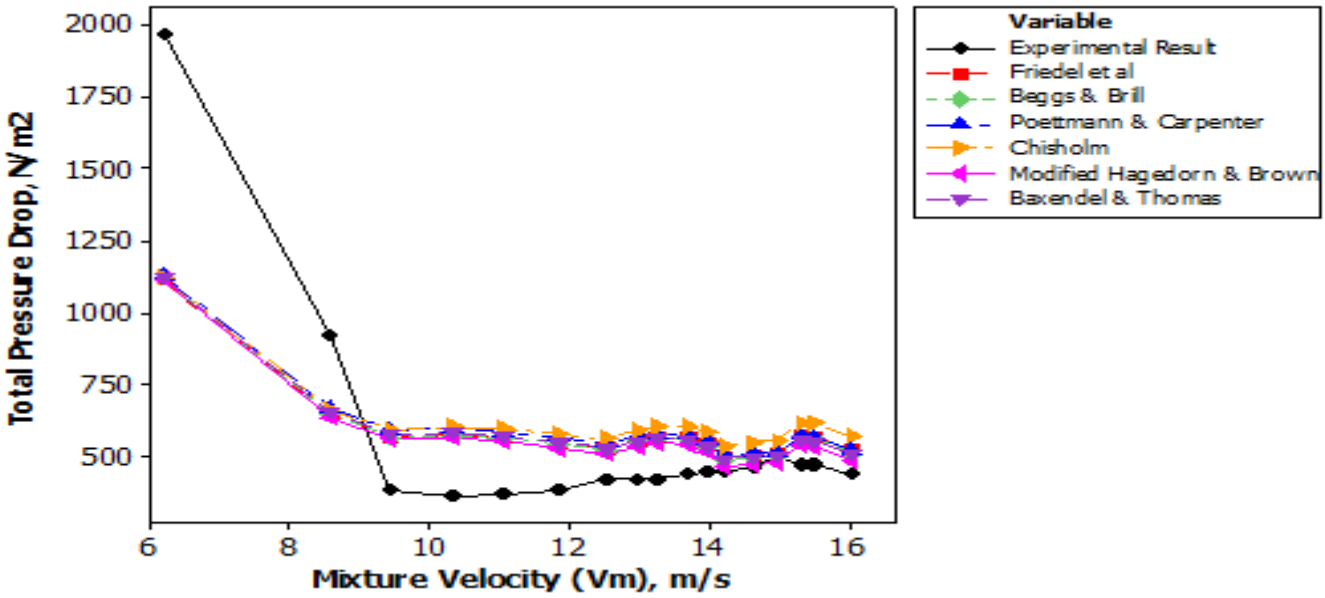

Figure (4.84): Comparison of experimental and calculated pressure drop result.

From Figure (4.84) three regions can be observed: At low mixture superficial velocity between 6.19-9.11m/s where all the empirical correlations under-predicts the experimental data; at intermediate mixture velocity of 9.11-14 m/s where all the correlations over-predicted the measured pressure drop; and at high mixture superficial velocity where the performance of the correlations were close to the measured result.

CHAPTER FIVE

CONCLUSION/RECOMMENDATION/FUTURE WORK

5.1 Conclusion

The main points and conclusion to be drawn from this can be summarized as follows:

- The effect of gas superficial velocity on the time-averaged pressure drop in the range of conditions studied in this work can be identified in two distinct regions, namely the lower gas superficial velocity region and the upper gas superficial velocity region. In the lower region between 3.45 m/s to 7 m/s the time-averaged pressure drop decreases sharply with an increase in gas superficial velocity whilst at higher gas superficial velocities the decrease is more gradual. On the other hand, the time-averaged pressure drop increases with an increase in liquid superficial velocity.
- The total pressure drop profile becomes less erratic (approaches a constant value) with time along the pipe length as the gas superficial velocity increases at constant liquid superficial velocity. In other words, the extent of fluctuation in the pressure drop grows as the gas flow-rates are reduced.
- There is a considerable effect of pipe diameter on frictional pressure drop. From the sensitivity analysis carried out, it can be noticed that the effect of pipe diameter on frictional pressure drop is more pronounced at a low diameter range between 0.0762 mm (3”) and 0.0381 mm (1”) especially for Poettmann and Carpenter (1952) correlation where the sensitivity is quite large. Hence diameter consideration should play an important role in flow design and optimization.
- Total pressure drop increases with an increase in liquid film fraction.

- The measured total pressure drop and the calculated total pressure drop follow the same trend. But all the six empirical correlations selected slightly over-predicted the total pressure drop. The modified Hagedorn and Brown (1964) correlation came closest to the experimental result while the largest over-prediction was observed with Chisholm (1973) correlation.

5.2 Recommendation

From the analysis carried out and the conclusion thereof, the modified Hagedorn and Brown (1964) is recommended to predict two-phase vertical pressure drop in the absence of an experimental work.

5.3 Future work

There are still a lot of work to be done in this complex area of research especially in large diameter pipes. From the results of this work the following areas of research for further work are recommended:

- Extend this work using fluids closer in terms of physical properties to those used in the oil and gas industry.
- Employing wider range of gas and liquid velocities in order to model exactly what happens in annular flow.

REFERENCE

Mohammed Zangana, (2011), "Film Behavior of Vertical Gas-Liquid Flow in a Large Diameter Pipe". Department of Chemical and Environmental Engineering, University of Nottingham, UK.

M.Zangana, G.P. Van der Meulen and B.J.Azzopardi (2010), "The Effect of Gas and Liquid Velocities on Frictional Pressure Drop in Two Phase Flow for Large Diameter Vertical Pipe". Process and Environmental Engineering Research Division, Faculty of Engineering, University of Nottingham, UK.

Gabor Takacs, (2001), "Considerations on the Selection of an Optimum Vertical Multiphase Pressure Drop Prediction Model for Oil Wells". University of Miskolc, Hungary.

Mars Khasanov, Rinat Khabibullin, Vitaly Krasnov, Alexander Pashali, and Slava Guk, (2007), "A Simple Mechanistic Model for Void Fraction and Pressure Gradient Prediction in Vertical and Inclined Gas/Liquid Flow". Rosneft Oil Company.

Poettmann and Carpenter (1952), "The Multi-phase Flow of Gas, Oil, and Water through Vertical Flow String with Application to the Design of Gas-lift Installations" Philips Company, Okla.

James P. Brill (University of Tulsa) and Hemanta Mukherjee (Shlumberger Oilfields, West and South Africa), (1999), "Multi-phase Flow in Wells"

G.J. Zabaras (1994), "Physical Modelling of Vertical Multiphase Flow Prediction of Pressure Gradients in Oil and Gas Wells" Shell Development Co. Texas, USA.

Khalid Aziz (University of Calgary, Alberta), **George W. Govier** (Alberta Energy Resources Conservation Board), **Maria Fogarasi** (University of Calgary Alberta), "Pressure Drop in Wells Producing Oil and Gas" (1972), Calgary Alberta.

George H. Fancher, Jr. and Kermit E. Brown (1963) "Prediction of Pressure Gradients for Multiphase Flow in Tubing" University of Texas, USA.

Alton R. Hagedorn and Kermit E. Brown (1965) "Experimental Study of Pressure Gradients Occurring During Continuous Two-Phase Flow in Small-Diameter Vertical Conduits". University of Texas, USA.

G. L. Chienci, *G.* M. Ciucci, and *G.* Sclocchi (1974), "Two-Phase Vertical Flow in Oil Wells– Prediction of Pressure Drop", AGIP Exploration & Production.

Peter Griffith, Chun Woon Lau, Pou Cheong Hon, and John F. Pearson, (1973)," Two Phase Pressure Drop in Inclined and Vertical Oil Wells", Department of Mechanical Engineering, M.I.T. ,Cambridge, Mass., U.S.A.

K.M. Reinicke, R. J. Remer and G. Hueni, (1987) "Comparison of Measured and Predicted Pressure Drops in Tubing for High-Water-Cut Gas Wells", SPE Production Engineering.

A. Rashid Hasan, (SPE, U. of North Dakota), **C. Shah Kabir,** (SPE, Schlumberger Overseas S.A), (1988), "A Study of Multiphase Flow Behavior in Vertical Wells"

R.I. Issa and Z.F. Tang, (1991) "Prediction of Pressure Drop and Hold-Up in Gas/Liquid Flow in Pipes Using the Two-Fluid Model". Mineral Resources Engineering, Imperial College, London, U.K.

J.K. Pucknell, J.N.E. Mason, and E.G. Vervest (1993) "An Evaluation of Recent Mechanistic Models of Multiphase Flow for Predicting Pressure Drops in Oil and Gas Wells". BP Exploration.

Musaab M. Ahmed and Mohammed A. Ayoub, (2004), "A Comprehensive Study on the Current Pressure Drop Calculation in Multiphase Vertical Wells; Current Trends and Future

Prospective", Petroleum Engineering Department, Faculty of Geosciences and Petroleum Engineering, Universiti Teknologi PETRONAS, Bandar Seri Iskandar, Malaysia.

G. J. Zabaras, "Physical Modelling of Vertical Multi-phase Flow: Prediction of Pressure Gradients in Oil and Gas Wells". Shell Development Company.

Kaji, R., Omebere-Iyari, N. K., Hernandez-Perez, V., and Azzopardi, B. J., (2007), "The Effect of Pipe Diameter on Flow Pattern in Vertical Up-flow", 6th Int. Conf Multiphase Flow, Leipzig, Germany.

Two Phase Flow Regimes in Reduced Gravity, NASA Lewis Research Center Motion Picture Directory 1704. By J. B. McQuillen, R. Vernon and A. E. Dukler. *www3.nd.edu/~mjm/flow.regimes.html*

NOMENCLATURE

Symbol	Description	Unit
A	Cross sectional area	m^2
D, d, d_o	Diameter of pipe	m
dL, dz	Change in length	m
ΔP_f	Frictional Pressure drop	N/ m^2
f/fn	Friction factor/ two phase friction factor	Dimensionless
g	Gravitational acceleration	m/s
Ku_g	Kutateladze number	Dimensionless
N_{Re}	Reynolds Number	Dimensionless
p	Pressure	N/m^2
q_g	Gas flow rate	m^3/s
q_L	Liquid flow rate	m^3/s
G_L	Liquid mass flux	Kg/ m^2s
G_G	Gas mass flux	Kg/ m^2s
U_M, V_m	Mixture superficial velocity	m/s
U_{SG}, V_{sg}	Gas superficial velocity	m/s
U_{SL}, V_{sl}	Liquid superficial velocity	m/s
x	Liquid quality,	dimensionless
M	Mass flow rate	Kg/s
$E,F,H,Fr,$ and We	Friedel's factors	dimensionless
$/ \Phi_{ch}$	Friedel's/Chisholm's two-phase multiplier	dimensionless
R/r	Pipe radius	m
$N_d, N_L, N_{LV},$ and N_{gv}	Duns and Ros dimensionless group	

GREEK SYMBOLS

λ_L	Liquid film fraction, dimensionless
ε	Gas void fraction dimensionless

μ_g	Gas viscosity	cP
μ, μ_L	Liquid viscosity	Kg/m.s
μ_m	Mixture viscosity	Kg/m.s
ρ_l	Liquid density	Kg/m^3
ρ_g	Gas density	Kg/m^3
ρ_m ,ρ_n	Density of the gas-liquid mixture	Kg/m^3
σ	Surface tension	N/m
φ	Factor to correct film fraction for pipe inclination	Dimensionless
C	Beggs and Brill dimensionless parameter	
τ	Wall shear stress	N/m^2

SUBSCRIPTS/SUPERSCRIPTS

H

Hydrostatic

$_f$, Fr

Frictional

a,b, and c

Correlations for horizontal liquid

holdup

e,f,g, and h

Correlation for C

Lo Liquid

only/Liquid phase

Go Gas

only/Gas phase

$_{G, g}$ Gas phase

APPENDIX A

CALCULATION PROCEDURES FOR SELECTED MODELS

Friedel Correlation:

The correlation method for Friedel (1979) utilizes a two-phase multiplier. The following steps were used in estimating the frictional pressure drop through Friedel correlation:

The dimensionless factors, W_e Fr, E, F and H are as follows:

Friedel's two-phase multiplier is:

Chisholm Correlation:

Chisholm's parameter B = 4.8 for mas flux G< 500 kg/m^{2}s

For Re > 2000

Chisholm's two-phase multiplier is calculated as:

Where n is the exponent from the frictional factor expression of Blasius (n = 0.25)

Beggs and Brill correlation:

The first step to calculating the pressure drop due to friction is to calculate the empirical parameter S. The value of S is governed by the following conditions:

Where are correlation constants for horizontal liquid hold-up (a, b and c are respectively 0.845, 0.5351 and 0.0173)

The factor to correct λ_L for the effect of pipe inclination is given by

Where e, f, g and h are correlations for C. The values of e, f, g and h are respectively 0.011, -3.768, 3.539 and -1.614.

since y < 1

Where is the normalizing friction factor which is derived from Drew et al equation given by

And f is the two phase friction factor

Modified Hagedorn and Brown

Equations for Duns and Ros dimensionless group

The pipe is assumed hydraulically smooth and the frictional factor is given by

Poettmann and Carpenter and Baxendel and Thomas

The values of were calculated and the following graph of frictional factor against was digitized used a digitizing software and the values of the corresponding frictional factor for every was derived.

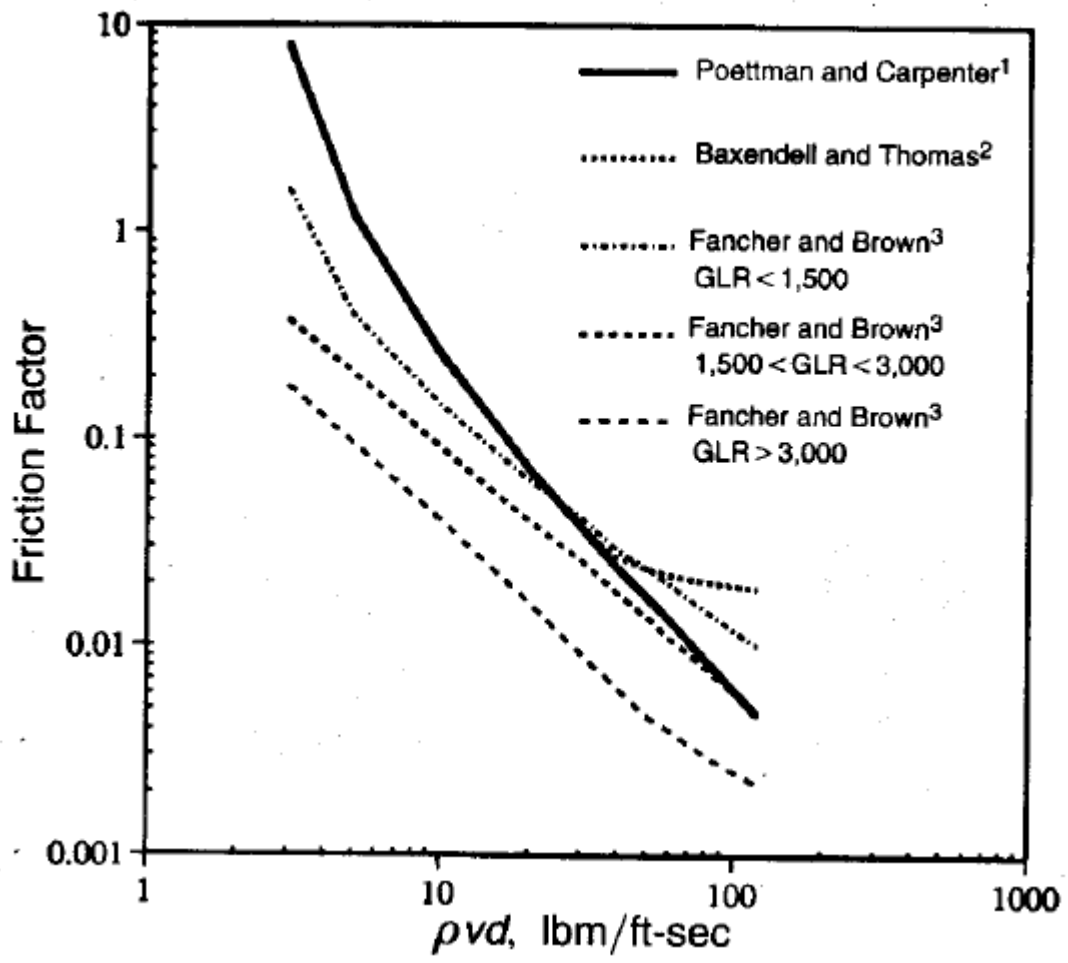

Figure A1: Friction factor chat for different empirical correlations.

APPENDIX B

Fluid and Pipe properties		
U_{sl}	0.02	m/s
ρ_g	3.55	kg/m^3
ρ_l	998	kg/m^3
μ_g	0.000018	kg/m.s
μ_l	0.00089	kg/m.s
D	0.0381	m
A_p	0.001140551	m^2
σ	0.072	N/m
g	9.81	m/s
L	1.64	m

Table B1: Fluid and Pipe geometric properties.

U_{sg} (m/s)	ε	HL	x	ρ_H	ML	MG	M	GL	GG	G	W_e	Fr	F	f_{to}	f_{Go}	E	Q_{Fr}^2	Re_L	Re_G	ΔP_L	ΔP_{Fr}	ΔP_H	ΔP_{Total}
6.17	0.9347	0.065	0.9401	3.775	0.00149	0.0234	0.0248	1.3034	20.473	21.777	66.47	89.03	0.4948	0.2868	0.00548	4.748	4.748	55.80	43334.9	11.730	55.70	1101.9	1157.55
8.56	0.9646	0.035	0.9765	3.635	0.00081	0.0334	0.0342	0.7066	29.312	30.019	131.17	182.44	0.3992	0.5290	0.00501	2.537	2.537	30.25	62044.3	41.118	104.32	623.5	727.80
9.42	0.9697	0.030	0.9817	3.616	0.00069	0.0370	0.0377	0.6048	32.428	33.033	159.68	223.28	0.3774	0.6180	0.00488	2.140	2.140	25.89	68638.7	58.168	124.48	541.9	666.37
10.31	0.9695	0.031	0.9831	3.611	0.00069	0.0405	0.0412	0.6088	35.484	36.093	190.92	267.34	0.3704	0.6139	0.00477	2.112	2.112	26.06	75108.2	68.990	145.73	545.1	690.82
11.05	0.9703	0.030	0.9847	3.605	0.00068	0.0434	0.0441	0.5928	38.062	38.655	219.33	307.60	0.3625	0.6305	0.00469	2.027	2.027	25.38	80565.5	81.265	164.76	532.3	697.05
11.83	0.972	0.028	0.9865	3.598	0.00064	0.0466	0.0472	0.5589	40.821	41.379	251.80	353.79	0.3521	0.6688	0.00461	1.885	1.885	23.93	86403.6	98.777	186.22	505.1	691.30
12.52	0.9733	0.027	0.9878	3.594	0.00061	0.0493	0.0499	0.5329	43.259	43.792	282.40	397.33	0.3438	0.7013	0.00454	1.777	1.777	22.81	91565.5	116.018	206.12	484.3	690.41
12.98	0.9718	0.028	0.9876	3.594	0.00064	0.0511	0.0517	0.5629	44.780	45.342	302.67	425.74	0.3454	0.6640	0.00450	1.859	1.859	24.10	94783.4	117.762	218.96	508.3	727.25
13.25	0.9713	0.029	0.9876	3.594	0.00065	0.0521	0.0528	0.5729	45.688	46.260	315.06	443.18	0.3452	0.6524	0.00448	1.883	1.883	24.52	96705.3	120.442	226.79	516.3	743.07
13.68	0.9716	0.028	0.9881	3.592	0.00065	0.0538	0.0545	0.5669	47.185	47.752	335.87	472.71	0.3418	0.6593	0.00444	1.850	1.850	24.27	99874.5	129.688	239.95	511.5	751.44
13.97	0.9732	0.027	0.9890	3.589	0.00061	0.0550	0.0557	0.5349	48.264	48.799	351.09	494.58	0.3356	0.6987	0.00442	1.739	1.739	22.90	102159.6	143.528	249.64	485.9	735.53
14.22	0.9762	0.024	0.9905	3.584	0.00054	0.0562	0.0567	0.4750	49.280	49.755	365.49	515.60	0.3250	0.7868	0.00440	1.541	1.541	20.34	104308.4	168.009	258.90	437.9	696.79
14.63	0.9759	0.024	0.9906	3.584	0.00055	0.0578	0.0584	0.4810	50.685	51.166	386.58	545.42	0.3239	0.7770	0.00437	1.550	1.550	20.59	107282.9	175.463	271.95	442.7	714.65
14.96	0.9756	0.024	0.9907	3.583	0.00056	0.0591	0.0596	0.4870	51.812	52.299	403.93	569.96	0.3231	0.7674	0.00434	1.561	1.561	20.85	109669.1	181.068	282.63	447.5	730.12
15.31	0.9719	0.028	0.9895	3.588	0.00064	0.0602	0.0609	0.5609	52.823	53.384	420.36	592.42	0.3323	0.6664	0.00432	1.785	1.785	24.01	111809.2	163.818	292.35	506.7	799.04
15.5	0.9723	0.028	0.9898	3.587	0.00063	0.0610	0.0617	0.5529	53.501	54.054	431.09	607.72	0.3303	0.6760	0.00431	1.755	1.755	23.67	113243.4	170.378	298.94	500.3	799.23
16.05	0.9755	0.025	0.9913	3.581	0.00056	0.0634	0.0640	0.4890	55.582	56.071	464.56	655.90	0.3183	0.7643	0.00427	1.542	1.542	20.93	117647.6	207.275	319.58	449.1	768.68

Usg (m/s)	ε	λ	V_m	ρ_n	μ_n	N_{Fr}	$H_{L(0)}$	N_{Lv}	C	ψ	$H_{L(\theta)}$	y	S	N_{Re}	fn	f	ΔP_F	ΔP_H	ΔP_{Total}
6.17	0.935	0.0653	6.19	68.5	7.49E-05	102.51	0.1811	48.963	-0.9672	0.7106	0.1287	3.942	0.501	215528	0.0154	0.0255	89.37678	1101.856	1191.232
8.56	0.965	0.0354	8.58	38.8	4.89E-05	196.96	0.129	67.929	-1.2579	0.6237	0.0805	5.465	0.568	259234	0.0149	0.0262	100.0889	623.4823	723.5712
9.42	0.97	0.0303	9.44	33.7	4.44E-05	238.42	0.1183	74.753	-1.334	0.6009	0.0711	5.991	0.589	272708	0.0147	0.0265	106.4705	541.8868	648.3574
10.31	0.97	0.0305	10.33	33.9	4.46E-05	285.5	0.1184	81.816	-1.3538	0.595	0.0704	6.147	0.595	299008	0.0144	0.0262	126.7073	545.0867	671.794
11.05	0.97	0.0297	11.07	33.1	4.39E-05	327.87	0.1164	87.688	-1.3798	0.5872	0.0684	6.353	0.603	317876	0.0143	0.0261	141.5237	532.2874	673.8111
11.83	0.972	0.028	11.85	31.4	4.24E-05	375.7	0.1126	93.878	-1.4164	0.5763	0.0649	6.655	0.615	334171	0.0141	0.0261	154.1508	505.0889	659.2396
12.52	0.973	0.0267	12.54	30.1	4.13E-05	420.73	0.1095	99.354	-1.4463	0.5673	0.0621	6.917	0.624	348378	0.014	0.0262	165.7915	484.29	650.0815
12.98	0.972	0.0282	13	31.6	4.26E-05	452.16	0.1126	103	-1.4367	0.5702	0.0642	6.838	0.621	367413	0.0139	0.0258	184.5767	508.2887	692.8654
13.25	0.971	0.0287	13.27	32.1	4.3E-05	471.14	0.1136	105.15	-1.4358	0.5705	0.0648	6.833	0.621	377086	0.0138	0.0257	194.3477	516.2883	710.636
13.68	0.972	0.0284	13.7	31.8	4.28E-05	502.17	0.1129	108.56	-1.4471	0.5671	0.064	6.935	0.625	388045	0.0137	0.0257	204.8793	511.4885	716.3678
13.97	0.973	0.0268	13.99	30.2	4.14E-05	523.65	0.1093	110.86	-1.4719	0.5597	0.0612	7.159	0.633	389123	0.0137	0.0259	204.5036	485.89	690.3936
14.22	0.976	0.0238	14.24	27.2	3.88E-05	542.53	0.1025	112.84	-1.5161	0.5464	0.056	7.583	0.648	381046	0.0138	0.0264	194.6128	437.8926	632.5054
14.63	0.976	0.0241	14.65	27.5	3.9E-05	574.22	0.1031	116.1	-1.5189	0.5456	0.0563	7.614	0.649	393657	0.0137	0.0262	207.1851	442.6924	649.8774
14.96	0.976	0.0244	14.98	27.8	3.93E-05	600.38	0.1037	118.72	-1.5203	0.5452	0.0565	7.63	0.65	404178	0.0136	0.0261	218.0086	447.4921	665.5006
15.31	0.972	0.0281	15.33	31.5	4.25E-05	628.77	0.1118	121.49	-1.4783	0.5577	0.0623	7.23	0.636	432787	0.0135	0.0254	251.6357	506.6888	758.3245
15.5	0.972	0.0277	15.52	31.1	4.22E-05	644.45	0.1109	123	-1.4862	0.5554	0.0616	7.306	0.638	436196	0.0134	0.0254	254.9653	500.2891	755.2545
16.05	0.976	0.0245	16.07	27.9	3.94E-05	690.94	0.1037	127.37	-1.5362	0.5404	0.056	7.801	0.656	434174	0.0135	0.0259	249.9004	449.092	698.9924

Usg (m/s)	ε	λ	V_m	ρ_n	$\rho_m V_m d$	f	ΔP_F	ΔP_H	ΔP_{Total}
6.17	0.9347	0.0653	6.19	68.4876	16.152	0.10828	623.3649	1101.86	1725.22
8.56	0.9646	0.0354	8.58	38.7535	12.6685	0.15748	985.6486	623.482	1609.13
9.42	0.9697	0.0303	9.44	33.6818	12.1141	0.16872	1111.062	541.887	1652.95
10.31	0.9695	0.0305	10.33	33.8807	13.3345	0.14551	1154.179	545.087	1699.27
11.05	0.9703	0.0297	11.07	33.0852	13.9542	0.13567	1206.78	532.287	1739.07
11.83	0.972	0.028	11.85	31.3946	14.1742	0.13244	1280.906	505.089	1785.99
12.52	0.9733	0.0267	12.54	30.1018	14.3819	0.1295	1344.846	484.29	1829.14
12.98	0.9718	0.0282	13	31.5935	15.6483	0.1137	1331.845	508.289	1840.13
13.25	0.9713	0.0287	13.27	32.0907	16.2246	0.10753	1333.113	516.288	1849.4
13.68	0.9716	0.0284	13.7	31.7924	16.5947	0.10385	1359.592	511.489	1871.08
13.97	0.9732	0.0268	13.99	30.2013	16.0978	0.10884	1411.434	485.89	1897.32
14.22	0.9762	0.0238	14.24	27.2179	14.7669	0.12433	1505.449	437.893	1943.34
14.63	0.9759	0.0241	14.65	27.5162	15.3586	0.11702	1516.163	442.692	1958.86
14.96	0.9756	0.0244	14.98	27.8146	15.8748	0.1112	1522.784	447.492	1970.28
15.31	0.9719	0.0281	15.33	31.494	18.3948	0.0886	1438.759	506.689	1945.45
15.5	0.9723	0.0277	15.52	31.0963	18.3876	0.08866	1456.902	500.289	1957.19
16.05	0.9755	0.0245	16.07	27.914	17.0908	0.09924	1569.528	449.092	2018.62

U_{sg} (m/s)	ε	λ_L	ρ_m	μ_m	M_L	M_G	M	G_L	G_G	G	Re_G	Re_L	fL	f_G	$(dP/dZ)_L$	$(dP/dZ)_G$	Y^2	x	Q_{ch}^2	$(dP/dZ)_{Fr}$	ΔP_F	ΔP_H	ΔP_{Total}
6.17	0.935	0.065	68.49	7.49E-05	0.00149	0.0234	0.0248	1.3034	20.47	21.777	43335	55.8	0.2868	0.00548	0.02562	33.9364	1324.4	0.5232	2312.03	59.2417	97.1564	1101.9	1199.01
8.56	0.965	0.035	38.75	4.89E-05	0.00081	0.0334	0.0342	0.7066	29.31	30.019	62044	30.25	0.529	0.00501	0.01389	63.5956	4578.3	0.6036	8178.94	113.611	186.322	623.48	809.804
9.42	0.97	0.03	33.68	4.44E-05	0.00069	0.037	0.0377	0.6048	32.43	33.033	68639	25.89	0.618	0.00488	0.01189	75.8918	6383.1	0.6262	11412.1	135.684	222.521	541.89	764.408
10.31	0.97	0.031	33.88	4.46E-05	0.00069	0.0405	0.0412	0.6088	35.48	36.093	75108	26.06	0.6139	0.00477	0.01197	88.8488	7423.9	0.6471	13252.7	158.607	260.116	545.09	805.202
11.05	0.97	0.03	33.09	4.39E-05	0.00068	0.0434	0.0441	0.5928	38.06	38.655	80566	25.38	0.6305	0.00469	0.01165	100.452	8619.5	0.6628	15347.5	178.861	293.332	532.29	825.619
11.83	0.972	0.028	31.39	4.24E-05	0.00064	0.0466	0.0472	0.5589	40.82	41.379	86404	23.93	0.6688	0.00461	0.01099	113.535	10334	0.6778	18332.5	201.419	330.327	505.09	835.416
12.52	0.973	0.027	30.1	4.13E-05	0.00061	0.0493	0.0499	0.5329	43.26	43.792	91566	22.81	0.7013	0.00454	0.01048	125.669	11995	0.6901	21198.4	222.093	364.232	484.29	848.522
12.98	0.972	0.028	31.59	4.26E-05	0.00064	0.0511	0.0517	0.5629	44.78	45.342	94783	24.1	0.664	0.0045	0.01107	133.5	12065	0.6978	21261.7	235.27	385.843	508.29	894.131
13.25	0.971	0.029	32.09	4.3E-05	0.00065	0.0521	0.0528	0.5729	45.69	46.26	96705	24.52	0.6524	0.00448	0.01126	138.273	12278	0.7021	21600.9	243.262	398.949	516.29	915.238
13.68	0.972	0.028	31.79	4.28E-05	0.00065	0.0538	0.0545	0.5669	47.18	47.752	99874	24.27	0.6593	0.00444	0.01114	146.3	13128	0.7087	23030.8	256.654	420.912	511.49	932.401
13.97	0.973	0.027	30.2	4.14E-05	0.00061	0.055	0.0557	0.5349	48.26	48.799	102160	22.9	0.6987	0.00442	0.01052	152.208	14474	0.713	25341.3	266.492	437.046	485.89	922.936
14.22	0.976	0.024	27.22	3.88E-05	0.00054	0.0562	0.0567	0.475	49.28	49.755	104308	20.34	0.7868	0.0044	0.00934	157.855	16903	0.7166	29542.9	275.899	452.475	437.89	890.367
14.63	0.976	0.024	27.52	3.9E-05	0.00055	0.0578	0.0584	0.481	50.68	51.166	107283	20.59	0.777	0.00437	0.00946	165.816	17534	0.7224	30557.7	288.973	473.916	442.69	916.608
14.96	0.976	0.024	27.81	3.93E-05	0.00056	0.0591	0.0596	0.487	51.81	52.299	109669	20.85	0.7674	0.00434	0.00957	172.324	17999	0.7268	31291.8	299.599	491.342	447.49	938.834
15.31	0.972	0.028	31.49	4.25E-05	0.00064	0.0602	0.0609	0.5609	52.82	53.384	111809	24.01	0.6664	0.00432	0.01103	178.252	16166	0.7314	28034	309.109	506.939	506.69	1013.63
15.5	0.972	0.028	31.1	4.22E-05	0.00063	0.061	0.0617	0.5529	53.5	54.054	113243	23.67	0.676	0.00431	0.01087	182.273	16770	0.7338	29039.4	315.637	517.644	500.29	1017.93
16.05	0.976	0.025	27.91	3.94E-05	0.00056	0.0634	0.064	0.489	55.58	56.071	117648	20.93	0.7643	0.00427	0.00961	194.858	20269	0.7406	34955.3	336.046	551.115	449.09	1000.21

Usg (m/s)	ε	λ	V_m	ρ_n	N_{LV}	N_{GV}	N_d	N_L	μ_s	N_{Re}	f	ΔP_F	ΔP_H	ΔP_{Total}
6.17	0.9347	0.0653	6.19	68.48759	0.420565	129.7443	1807.293	0.000376	2.32219E-05	2318504	0.008104	13.997	1101.86	1115.85
8.56	0.9646	0.0354	8.58	38.75353	0.420565	180.0019	1807.293	0.000376	2.06654E-05	2043421.8	0.008364	15.705	623.482	639.19
9.42	0.9697	0.0303	9.44	33.68184	0.420565	198.0862	1807.293	0.000376	2.02584E-05	1993274.9	0.008416	16.626	541.887	558.51
10.31	0.9695	0.0305	10.33	33.88073	0.420565	216.8013	1807.293	0.000376	2.02742E-05	2192369	0.008218	19.555	545.087	564.64
11.05	0.9703	0.0297	11.07	33.08516	0.420565	232.3622	1807.293	0.000376	2.0211E-05	2301425.1	0.008119	21.666	532.287	553.95
11.83	0.972	0.028	11.85	31.3946	0.420565	248.7643	1807.293	0.000376	2.00774E-05	2353256.3	0.008074	23.427	505.089	528.52
12.52	0.9733	0.0267	12.54	30.10181	0.420565	263.2738	1807.293	0.000376	1.99759E-05	2399874.3	0.008034	25.031	484.29	509.32
12.98	0.9718	0.0282	13	31.59349	0.420565	272.9468	1807.293	0.000376	2.00931E-05	2595960.4	0.007878	27.685	508.289	535.97
13.25	0.9713	0.0287	13.27	32.09071	0.420565	278.6244	1807.293	0.000376	2.01323E-05	2686336.2	0.007811	29.052	516.288	545.34
13.68	0.9716	0.0284	13.7	31.79238	0.420565	287.6666	1807.293	0.000376	2.01088E-05	2750818.2	0.007765	30.496	511.489	541.98
13.97	0.9732	0.0268	13.99	30.20126	0.420565	293.7648	1807.293	0.000376	1.99837E-05	2685169.1	0.007812	30.392	485.89	516.28
14.22	0.9762	0.0238	14.24	27.21791	0.420565	299.0218	1807.293	0.000376	1.97512E-05	2492160.4	0.007959	28.912	437.893	466.80
14.63	0.9759	0.0241	14.65	27.51625	0.420565	307.6434	1807.293	0.000376	1.97743E-05	2588986.4	0.007883	30.642	442.692	473.33
14.96	0.9756	0.0244	14.98	27.81458	0.420565	314.5827	1807.293	0.000376	1.97974E-05	2672877.6	0.007821	32.129	447.492	479.62
15.31	0.9719	0.0281	15.33	31.49405	0.420565	321.9426	1807.293	0.000376	2.00852E-05	3052791.3	0.007565	36.854	506.689	543.54
15.5	0.9723	0.0277	15.52	31.09626	0.420565	325.938	1807.293	0.000376	2.00539E-05	3056357.2	0.007563	37.285	500.289	537.57
16.05	0.9755	0.0245	16.07	27.91403	0.420565	337.5035	1807.293	0.000376	1.98052E-05	2876495.4	0.007679	36.432	449.092	485.52

Usg (m/ s)	ε	λ	V_m	ρ_n	$\rho_m V_m d$	f	ΔP_F	ΔP_H	ΔP_{Total}
6.17	0.9347	0.0653	6.19	68.48759	53.8401	0.013038	22.51932	1101.856	1124.375
8.56	0.9646	0.0354	8.58	38.75353	42.2282	0.01735	32.57771	623.4823	656.06
9.42	0.9697	0.0303	9.44	33.68184	40.3805	0.018287	36.12644	541.8868	578.0133
10.31	0.9695	0.0305	10.33	33.88073	44.4485	0.016335	38.87021	545.0867	583.9569
11.05	0.9703	0.0297	11.07	33.08516	46.5141	0.015485	41.32302	532.2874	573.6104
11.83	0.972	0.028	11.85	31.3946	47.2473	0.015203	44.11307	505.0889	549.202
12.52	0.9733	0.0267	12.54	30.10181	47.9395	0.014945	46.56233	484.29	530.8524
12.98	0.9718	0.0282	13	31.59349	52.1609	0.013533	47.5587	508.2887	555.8474
13.25	0.9713	0.0287	13.27	32.09071	54.0822	0.01297	48.23838	516.2883	564.5266
13.68	0.9716	0.0284	13.7	31.79238	55.3156	0.01263	49.60423	511.4885	561.0928
13.97	0.9732	0.0268	13.99	30.20126	53.6595	0.01309	50.92596	485.89	536.8159
14.22	0.9762	0.0238	14.24	27.21791	49.223	0.014488	52.62931	437.8926	490.5219
14.63	0.9759	0.0241	14.65	27.51625	51.1953	0.013834	53.77153	442.6924	496.4639
14.96	0.9756	0.0244	14.98	27.81458	52.9161	0.013306	54.66378	447.4921	502.1559
15.31	0.9719	0.0281	15.33	31.49405	61.3161	0.01119	54.50902	506.6888	561.1978
15.5	0.9723	0.0277	15.52	31.09626	61.292	0.011195	55.18842	500.2891	555.4776
16.05	0.9755	0.0245	16.07	27.91403	56.9695	0.0122	57.88449	449.092	506.9765